https://doi.org/10.5194/acp-2020-491
Preprint. Discussion started: 16 June 2020


Atmospheric Chemistry and Physics Discussions

# Spatiotemporal variability of elemental and organic carbon in Svalbard snow during 2007–2018.

Christian Zdanowicz[1], Jean-Charles Gallet[2], Mats P. Björkman[3], Catherine Larose[4], Thomas Schuler[5], Bartłomiej Luks[6], Krystyna Koziol[7], Andrea Spolaor[8], Elena Barbaro[8,9], Tõnu Martma[10], Ward van Pelt[1], Ulla Wideqvist[11] and Johan Ström[11].

[1]Department of Earth Sciences, Uppsala University, Uppsala, 752 36, Sweden
[2]Norwegian Polar Institute, Tromsø, NO-9296, Norway
[3]Department of Earth Sciences, University of Gothenburg, 405 30 Gothenburg, Sweden
[4]Environmental Microbial Genomics, École Centrale de Lyon, Université de Lyon, 69134 Ecully, France
[5]Department of Geosciences, University of Oslo, 0316 Oslo, Norway
[6]Institute of Geophysics, Polish Academy of Sciences, 01-452 Warszawa, Poland
[7]Department of Analytical Chemistry, Gdańsk University of Technology, 80-233 Gdańsk, Poland
[8]Institute of Polar Sciences, ISP-CNR, 30170 Venice Mestre, Italy
[9]Department of Environmental Sciences, Informatics and Statistics, Ca' Foscari University of Venice, 30172 Mestre, Italy
[10]Department of Geology, Tallinn University of Technology, 19086 Tallinn, Estonia
[11]Department of Environmental Science, Stockholm University, 106 91 Stockholm, Sweden

*Correspondence to*: Christian Zdanowicz (christian.zdanowicz@geo.uu.se)

**Abstract.**

Light-absorbing carbonaceous aerosols emitted by biomass or fossil fuel combustion can contribute to amplify Arctic climate warming by lowering the albedo of snow. The Svalbard archipelago, being near to Europe and Russia, is particularly affected by these pollutants, and improved knowledge of their distribution in snow is needed to assess their impact. Here we present and synthesize new data obtained on Svalbard between 2007 and 2018, comprising 324 measurements of elemental (EC) and organic carbon (OC) in snow from 49 sites. We used these data, combined with meteorological and aerosol data and snowpack modelling, to investigate the variability of EC and OC deposition in Svalbard snow across latitude, longitude, elevation and time. Overall, EC concentrations ($C_{snow}^{EC}$) ranged from <1.0 to 266.6 ng g$^{-1}$, while OC concentrations ($C_{snow}^{OC}$) ranged from <1.0 to 9449.1 ng g$^{-1}$, with the highest values observed near Ny-Ålesund. Calculated snowpack loadings ($L_{snow}^{\mathrm{EC}}$, $L_{snow}^{\mathrm{OC}}$) in April 2016 were 0.1 to 16.2 mg m$^{-2}$ and 1.7 to 320.1 mg m$^{-2}$, respectively. The median $C_{snow}^{EC}$ and $L_{snow}^{EC}$ in the late 2015–16 winter snowpack on glaciers were close to or lower than those found in earlier (2007–09), comparable surveys. Both $L_{snow}^{EC}$ and $L_{snow}^{OC}$ increased exponentially with elevation and snow accumulation, with dry deposition likely playing a minor role. Estimated area-averaged snowpack loads across Svalbard were 1.8 mg EC m$^{-2}$ and 71.5 mg OC m$^{-2}$ in April 2016. An ~11-year long dataset of spring surface snow measurements from central Brøgger Peninsula was used to quantify the interannual variability of EC and OC deposition in snow. On average, $C_{snow}^{EC}$ and $C_{snow}^{OC}$ at Ny-Ålesund (50 m a.s.l.) were 3 and 7 times higher, respectively, than on the nearby Austre Brøggerbreen glacier (456 m a.s.l.), and the median EC/OC in Ny-Ålesund was 6 times higher, pointing to some local EC emission from Ny-Ålesund. While no long-term trends between 2011 and 2018 were found, $C_{snow}^{EC}$ and $C_{snow}^{OC}$ showed synchronous variations at Ny-Ålesund and Austre Brøggerbreen. Comparing $C_{snow}^{EC}$ at Austre

https://doi.org/10.5194/acp-2020-491
Preprint. Discussion started: 16 June 2020


Atmospheric Chemistry and Physics Discussions

Brøggerbreen with aerosol data from Zeppelin Observatory, we found that snowfall washout ratios between 10 and 300 predict a range of $C_{snow}^{EC}$ in agreement with that measured in surface snow. Together, results from this study and comparable surveys confirm the existence of a longitudinal gradient in EC deposition across the Arctic and sub-Arctic, with the lowest $C_{snow}^{EC}$ found in the western Arctic (Alaska, Yukon) and central Greenland, and the highest in northwestern Russia and Siberia.

## 1 Introduction

Light-absorbing carbonaceous aerosols, such as black carbon (BC) or "brown carbon" (BrC; organic) that are transported to Arctic latitudes can lower the albedo of snow/ice-covered surfaces on which they are deposited, thereby enacting a positive feedback that amplifies climate warming (Bond et al., 2013). The Svalbard archipelago, owing to its proximity to the European and Russian mainland, is particularly affected by BC and BrC emissions from fossil fuel combustion (FF; heating, gas flaring, etc.) and biomass burning (BB; e.g., agricultural or forest fires). Source attribution using carbon isotopes and atmospheric transport modelling indicates that BC associated with pollution haze events at the Zeppelin Observatory on Spitsbergen include both BB and FF contributions, the latter being proportionally more important in winter than summer (Winiger et al., 2015, 2019). Quantifying the impact of BC deposition on the Arctic surface albedo requires knowledge of its concentrations, spatial distribution and variability in snow and ice. These data may also serve to verify the efficacy of ongoing and future measures to curb emissions of short-lived climate forcing aerosols, such as BC, that impact the Arctic (AMAP, 2015; Stohl et al., 2015). On Svalbard, reconnaissance surveys of BC in snow were carried out in 1984–85 by Noone and Clark (1988) and in 2007 by Doherty et al. (2010). This was followed in 2007–09 by more detailed investigations of the distribution of BC across the archipelago (Forsström et al., 2009, 2013). Localized studies have also been carried out near Longyearbyen (Aamaas et al, 2011; Khan et al., 2017) and Ny-Ålesund (Sihna et al., 2018; Jacobi et al., 2019). In addition, two ice cores recovered from the Lomonosovfonna and Holtedahlfonna icefields (Spitsbergen) have provided insights into longer-term variations in BC deposition on Svalbard (Ruppel et al., 2014, 2017; Osmont et al., 2018).

Here we present and synthesize new observational data which document the variability of BC in snow across Svalbard in terms of latitude, longitude, altitude and time. These data were gathered through field investigations conducted between 2007–18 on both Spitsbergen and Nordaustlandet (**Fig. 1**). The two main datasets consist of a spatial survey carried out across 22 glacier sites in April 2016, and an 11-year long series of surface snow observations made on central Brøgger Peninsula on northwestern Spitsbergen. The April 2016 survey included some of the sites previously visited in 2007–09 by Forsström et al. (2009, 2013), thus allowing for comparisons after a ~decadal interval. All data presented in this study were obtained by the thermo-optical transmittance method (TOT), which quantifies separately the more refractory and volatile carbon mass fractions present in particulate material filtered from melted snow (Chow et al., 2004; see below). Following Petzold et al. (2013), we designate the more refractory mass fraction as elemental carbon (EC) and the more volatile fraction as organic carbon (OC). In this paper, we use the new datasets, combined with meteorological and aerosol data and snowpack modelling, to (i) describe the spatial distribution of EC and OC deposited on Svalbard glaciers, (ii) estimate their mass loading in the winter snowpack

https://doi.org/10.5194/acp-2020-491
Preprint. Discussion started: 16 June 2020

Atmospheric Chemistry and Physics
Discussions

and how it relates to spatial variations in snow accumulation, (iii) describe the interannual variability of EC and OC concentration in snow on Brøgger Peninsula between 2007 and 2018, and (iv) constrain plausible estimates of the snowfall washout ratio for EC. Lastly, we place our findings in a broader pan-Arctic perspective by comparison with a compilation of published data obtained between 2002 and 2018 by comparable methods.

## 2 Material and methods

### 2.1 Field sampling

#### 2.1.1. April 16 survey

Part of the dataset presented here was produced following a comprehensive, coordinated survey of the physical, chemical and microbiological properties of the Svalbard seasonal snowpack carried out at the end of the 2015–16 winter by individuals from multiple institutions (see acknowledgments). In total, 22 sites were sampled between 4 and 29 April 2016 on 7 glaciers of Spitsbergen and Nordaustlandet (**Fig. 1**). Snowpits were sampled at three different elevations in the upper, middle and lower reaches of each glacier (**Table S1**), the snow depth increasing with altitude (e.g., Pramanik et al., 2019). Glacier sites were targeted partly for logistical reasons (ease of access by snowmobile), but also because sampling supraglacial snow avoided the heterogeneities in snow properties that may arise from interactions with vegetation and/or different substrates (e.g., wet vs. dry tundra soils). In addition, the selected glacier sites were at elevations of 102 to 1193 m a.s.l., which span ~65 % of the maximum relief in Svalbard (1713 m; **Fig. 2**).

In advance of the field campaign, standardized protocols were developed for the measurement of important snow physical properties (e.g., density, temperature) and the collection of samples for a variety of analyses, including EC, OC, and stable oxygen isotope ratios ($\delta^{18}O$). These protocols are documented in Gallet *et al.* (2018), and details relevant for this paper summarized hereafter. Snow sampling was performed in snowpits excavated down to the hard, icy firn surface representing the previous year's late summer ablation surface (in the accumulation zone of glaciers), or to the underlying bare ice surface (in the ablation zone). All snowpits were located well away from point sources of contamination (e.g., field camps), were accessed by foot from at least 100 m, and personnel doing the sampling wore protective, non-particulating suits, gloves, and face masks, and employed pre-cleaned plastic or stainless steel tools. The snow accumulation of each snowpit ($h_{\mathrm{SWE}}$, in water equivalent; w.e.) was calculated from discrete density measurements. After recording the physical properties of snow strata, large volume snow samples (~5 L each) were collected from the top 5 cm of the snowpack, and, where snowpack depth allowed for it, at 50-cm depth intervals beneath. The near-surface samples were collected to quantify EC and OC concentrations in snow ($C_{snow}^{EC}$ and $C_{snow}^{OC}$) at depths where light absorption by carbonaceous particles has the largest impact on snow albedo (Marks and King, 2013). The deeper samples were used to estimate the total column mass loading of EC and OC ($L_{snow}^{EC}$, $L_{snow}^{OC}$) in the seasonal snowpack. Quantification of $C_{snow}^{EC}$ and $C_{snow}^{OC}$ in layers from discrete snowfall events was not feasible, owing to the large snow volume required to achieve a sufficient particulate carbon mass for TOT analysis. All snow samples

https://doi.org/10.5194/acp-2020-491
Preprint. Discussion started: 16 June 2020




were double-bagged in sterile low-density polyethylene bags and returned frozen to a location where they were subsequently melted and filtered. Depending on logistics, this was done either at the Polish Polar Station Hornsund operated by the Polish Academy of Sciences, or at the Norwegian Polar Institute (NPI) facilities in Ny-Ålesund (Sverdrup station), Longyearbyen (UNIS) or Tromsø. A total of 89 samples were obtained from all 22 sites.

Analysis of downscaled ERA Interim climatological fields (Dee et al., 2011) over Svalbard show that surface temperatures in the 2015–16 winter exceeded the 30-year climatological normals for the 1981–2010 period by 2 to 6 °C, with the largest anomalies observed in the northeastern part of the archipelago (**Fig. S1a**). Total winter precipitation also exceeded 1981–2010 normals by 0.2 to 0.7 m w.e. over much of central and northern Spitsbergen (**Fig. S1b**). These unusual conditions arose partly owing to an extreme winter warming and precipitation event associated with a southerly air intrusion over Spitsbergen that occurred in late December 2015 (Binder et al., 2017; Kim et al., 2017; Maturilli et al., 2017). The implications of these climatological circumstances for the interpretation of our snow survey data are discussed later.

### 2.1.2. Surface snow monitoring, Brøgger Peninsula

In addition to the April 2016 survey, we report measurements of $C_{snow}^{EC}$ and $C_{snow}^{OC}$ in surface layers sampled by NPI staff from three sites on Brøgger Peninsula between 2007 and 2018 (**Fig. S2**). The first of these sites is in the accumulation zone of Austre Brøggerbreen (78.87° N, 11.92° E, 456 m a.s.l.), which was accessed by snowmobile from Ny-Ålesund. The other sites are in the outskirts of Ny-Ålesund, one ~80 m southeast of NPI's Sverdrup station (78.92° N, 11.93° E, ~50 m a.s.l.), the other near the Gruvebadet Atmospheric Laboratory (78.92° N, 11.89° E, ~50 m a.s.l.). Sampling was carried out at approximately weekly intervals by the NPI permanent staff at Sverdrup station, whenever their work schedule made it possible, and when safe snowmobile driving conditions (e.g., proper visibility, firm surface) allowed access to Austre Brøggerbreen. Because of these restrictions, the snow samples could not always be collected immediately after snow fall events. Over the ~11-year period considered, a total of 201 samples were collected between February and June, 86 % of which were taken in the spring months (March–May), April being the most represented month ($n$ = 44). Methods for field sample collection were the same as those described above for the April 2016 survey. Sample collection was limited to the top 5 cm of the snowpack (occasionally deeper). These data provide long-term estimates of the interannual variability of $C_{snow}^{EC}$ and $C_{snow}^{OC}$ in Svalbard against which results of the April 2016 survey (and others) can be compared.

We also report additional $C_{snow}^{EC}$ and $C_{snow}^{OC}$ measurements in snow collected on 6 glaciers in northwestern Spitsbergen ($n$ = 34; **Table S2**). These samples were collected irregularly, on an opportunistic basis, by NPI staff during other field research activities, but were handled and analyzed in the same manner as all those previously described. Altogether, the dataset presented here comprises a total of 324 measurements of $C_{snow}^{EC}$ and $C_{snow}^{OC}$ from 49 separate sites across Svalbard.

https://doi.org/10.5194/acp-2020-491
Preprint. Discussion started: 16 June 2020


Atmospheric Chemistry and Physics
Discussions

### 2.2 EC and OC analyses

All snow samples used in this study were processed in the same way: they were first melted at room temperature and the meltwater was filtered through pre-ashed, 47-mm diameter quartz microfiber filters, following the procedure described in Forsström *et al.* (2009). The filters were then air-dried at room temperature overnight, stored in sterile petri dishes, and later sent to the Department of Environmental Science of Stockholm University. There, EC/OC analysis was performed using a Sunset Laboratory carbon aerosol analyzer (Sunset Laboratory Inc., Forest Grove, USA), following the European Supersites for Atmospheric Aerosol Research thermal evolution protocol (EUSAAR_2; Cavalli *et al.*, 2010). A 1 x 1 cm$^2$ square section was used from each filter to determine separately the particulate EC and OC mass loading on each filter ($L_{filt}^{EC}$, $L_{filt}^{OC}$), from which their mass concentrations in snow ($C_{snow}^{EC}$, $C_{snow}^{OC}$) were calculated based on the volume of meltwater filtered. Blank filters ($n$ = 6) had particulate carbon loadings below the limit of detection (LOD) of the carbon analyzer, so no blank correction was applied to the data. The coefficient of variation (CV) on $C_{snow}^{EC}$ and $C_{snow}^{OC}$ was estimated to be ~40 % (see Supplement for details).

The presence of mineral dust particles in snow can lead to understimations of $C_{snow}^{EC}$ relative to $C_{snow}^{OC}$ by the TOT method (Wang et al., 2012; Lim et al., 2014). A total of 31 snow filters obtained from 7 glaciers surveyed in April 2016 (35 % of samples) were found to have faint to pronounced yellow-pink or grey-brown coloration, likely indicating the presence of k-feldspars and/or oxides which are commonly found in cryoconites, although carbonates may also be present on these filters (see notes in Supplemental dataset). The samples that produced the colored filters were typically found in snow layers near the base of snowpits, suggesting windblown dust dispersion and deposition in the autumn when the ground is only partially snow-covered. In 11 of the colored filters, the measured $L_{filt}^{EC}$ were noticeably lower than in filters from snow layers immediately above, and in 6 filters the $L_{filt}^{EC}$ was < LOD, possibly due to the effect of dust on TOT measurements. Some surface snow filters obtained from Sverdrup or Gruvebadet near Ny-Ålesund between 2010 and 2018 also showed coloration indicating the probable presence of windblown dust. Correcting for the effects of dust on the OC-EC split point of individual TOT thermograms is feasible, but it requires experimental data which we did not have (e.g., Wang et al., 2012). Therefore, no such corrections were applied to $C_{snow}^{EC}$ and $C_{snow}^{OC}$ data. We acknowledge, however, that the $C_{snow}^{EC}$ in snow samples that contained visible dust may be underestimated.

For the snowpits excavated on glaciers in April 2016, we computed mass loadings of EC ($L_{snow}^{EC}$) and OC ($L_{snow}^{OC}$) in the seasonal snowpack following:

$$L_{snow}^{EC} = \sum_{i=1}^{2} (C_{snow}^{EC})_i \rho_i z_i \tag{1}$$

https://doi.org/10.5194/acp-2020-491
Preprint. Discussion started: 16 June 2020

Atmospheric Chemistry and Physics Discussions

$$L^{OC}_{snow} = \sum_{i=1}^{n} (C^{OC}_{snow})_i \rho_i z_i \quad (2)$$

where $L^{EC}_{snow}$ and $L^{OC}_{snow}$ are in mg m$^{-2}$, $\rho_i$ is the mean density of snow layer $i$, $z_i$ its thickness, and $n$ the number of discrete layers. For samples which yielded $C^{EC}_{snow}$ <1 ng g$^{-1}$ we assigned a value of 0.5 ng g$^{-1}$ (half the LOD) in order to compute snowpack loadings (see below). An estimated error on individual density measurements ($\sigma_\rho$) of ± 6 % was used (Conger and McClung, 2009; Proksch et al., 2016), and the meter-scale variability of snow layer density at spatial scales of 1 to 100 m$^2$ was assumed to be on the order of 5 %, after Koenig et al. (2016). Combining uncertainties on $C^{EC}_{snow}$ and $C^{OC}_{snow}$ with these errors yields a median CV of ~30 % for $L^{EC}_{snow}$ and $L^{OC}_{snow}$ ($n$ = 22 snowpits).

### 2.3 $\delta^{18}$O analyses

The stable isotope ratio of oxygen ($^{16}$O:$^{18}$O) in snowpit samples collected in April 2016 was used to detect evidence of warming events associated with large autumn or winter snowfalls, that could help to interpret the $L^{EC}_{snow}$ and $L^{OC}_{snow}$ data. The measurements were made at the Institute of Geology of Tallinn's University of Technology, Estonia, using a Picarro model L2120-i water isotope analyzer (Picarro Inc., Sunnyvale, USA) (Lis et al., 2008). Results are reported in the standard delta notation $\delta^{18}$O relative to the Vienna Standard Mean Ocean Water. The analytical precision was ±0.1 ‰.

### 2.4 Supporting data

#### 2.4.1 Surface meteorological observations

Automated weather stations (AWS) were operated on 6 glaciers sampled during the April 2016 survey (**Table S3**). These stations were situated close to the estimated equilibrium line altitude (ELA) of the glaciers, and provided hourly recordings of air temperature and ultrasonic soundings of snow surface height changes that were used to interpret snowpit stratigraphic data, in particular the timing of snow accumulation and of snowmelt events. Data from the AWSs were supplemented with records from Longyearbyen and the airport in Ny-Ålesund obtained from the Norwegian Meteorological Institute, and from the Polish Polar Station Hornsund (N 77.00°, E 15.11°, 9 m a.s.l.).

#### 2.4.2 Snowpack modeling

Owing to the scarcity of direct precipitation measurements across Svalbard, reconstructing the snowpack accumulation history is challenging, and estimates from snowpits, probing and radar can only fill some of the spatial and temporal gaps. This difficulty can be partly circumvented by using the output of a snowpack model forced with meteorological observations (e.g., Jacobi et al., 2019). In this study, we use a coupled energy balance-snow model (van Pelt et al., 2012), which has recently been employed to investigate glacier and snow conditions across Svalbard (van Pelt et al., 2019). The model includes subroutines

https://doi.org/10.5194/acp-2020-491
Preprint. Discussion started: 16 June 2020


for the surface energy balance as well as internal snowpack processes (e.g., densification, melt-freeze events) that makes it possible to simulate the evolution of the seasonal snowpack (thickness and internal structure) for individual 1x1 km grid cells over Svalbard. The snow model routine simulates subsurface density, temperature and water content, while accounting for vertical water transport, liquid water storage, refreezing and runoff (Marchenko et al. 2017; Van Pelt et al. 2019). Fresh snow density is described by a temperature- and wind-dependent function (Van Kampenhout et al. 2017), while snow densification is the sum of destructive metamorphism, compaction by overburden pressure and compaction by drifting snow (Vionnet et al. 2012). Snow scouring and redistribution by wind is not accounted for, however. Layered snow properties are modelled with a vertical resolution of 1 cm.

Here, we used the model to simulate the snowpack evolution at some of the sites sampled during the April 2016 survey. For the April 2016 survey snowpits, simulations were limited to those sites located close to or above the local ELA (**Table S1**). As in van Pelt et al. (2019), the model was forced with downscaled, 3-hourly meteorological fields generated with the High Resolution Limited Area Model (HIRLAM, version 6.4.2; Reistad et al., 2009). For all modelled sites, precipitation was locally calibrated (scaled with a factor) to assure matching modelled and observed snow depths at the time of observation (April 2016). The snowpack model was also used to characterize the spatial variability of the seasonal snow cover over Brøgger Peninsula for the period 2008–18 during which surface snow was sampled for EC and OC (**Fig. S3**).

### 2.4.3 Black carbon aerosol measurements

The atmospheric mixing ratio of BC above Svalbard follows a well-defined seasonal cycle, peaking in late winter and early spring (Eleftheriadis et al., 2009). To establish how the timing of surface snow sample collection on Brøgger Peninsula compares with this seasonal cycle, and also to estimate BC washout ratios, we obtained aerosol data from the Zeppelin Observatory (N 78° 54.43', E 11° 53.20', 474 m a.s.l.), 2 km south of Ny-Ålesund, over the period 2007–18. The data used are filter-based measurements of the hourly mean aerosol light absorption coefficient ($\sigma_{ap}$) made with a Particle Soot Absorption Photometer (PSAP; $\lambda$ = 525 nm; Bond et al., 1999) or an aethalometer ($\lambda$ = 880 nm; Eleftheriadis et al., 2009). These data were used to calculate the hourly BC mass-equivalent mixing ratio in air ($C_{air}^{eBC}$, in ng m$^{-3}$; Petzold et al., 2013), following:

$$C_{air}^{eBC} = \frac{C_f \times \sigma_{ap}}{\mathrm{MAC}_\lambda} \times 10^9 \quad (3)$$

where $\sigma_{ap}$ is in m$^{-1}$, MAC$_\lambda$ is the wavelength-specific BC aerosol mass absorption coefficient cross-section (m$^2$ g$^{-1}$), and $C_f$ = 3.45 is a unitless correction factor accounting for light absorption in the filter matrix (Backman et al., 2017). We used an MAC$_{525}$ value of 12.5 m$^2$ g$^{-1}$ for the PSAP data, and a MAC$_{880}$ value of 15.9 m$^2$ g$^{-1}$ for the aethalometer data, after Eleftheriadis et al. (2009) and Sinha et al. (2017).

https://doi.org/10.5194/acp-2020-491
Preprint. Discussion started: 16 June 2020



## 3 Results

Descriptive statistics of $C_{snow}^{EC}$ and $C_{snow}^{OC}$ for all samples analyzed in this study are summarized in **Table 2**. The probability distributions of $C_{snow}^{EC}$ and $C_{snow}^{OC}$ both have skewness >4, therefore we use medians ($\tilde{C}_{snow}^{EC}$, $\tilde{C}_{snow}^{OC}$) as measures of their central tendency, but also report arithmetic and geometric means for comparisons with other published data. As both $C_{snow}^{EC}$ and $C_{snow}^{OC}$ are left-censored by the analytical LOD, the median and mean were estimated by replacing values < 1 ng g$^{-1}$ with 0.5 x LOD (0.5 ng g$^{-1}$), following Hornung and Reed (1990), while the geometric mean was estimated by the beta factor method of Ganser and Hewett (2010). Values of $C_{snow}^{EC}$ and $C_{snow}^{OC}$ < LOD are, however, included in plots (see below) to provide an as complete as possible description of our data. Overall, $C_{snow}^{EC}$ ranged from <1.0 to 266.6 ng g$^{-1}$, while $C_{snow}^{OC}$ ranged from <1.0 to 9449.1 ng g$^{-1}$. The highest $C_{snow}^{EC}$ (>50 ng g$^{-1}$) were measured in spring surface snow near Ny-Ålesund (Sverdrup and Gruvebadet sites). The $\tilde{C}_{snow}^{EC}$ at these two sites over the period 2007–18 (9.7 ng g$^{-1}$) was ~4 times higher than in surface layers at glacier sites (2.4 ng g$^{-1}$). At most sampling sites, EC accounted for <30 % (most typically, <5 %) of the total mass of particulate carbon (EC+OC) in snow, except near Ny-Ålesund, where it accounted for up to 61 %. The ratio of $C_{snow}^{EC}$ to $C_{snow}^{OC}$ (hereafter: EC/OC) in samples from glaciers varied from <0.01 to 0.43, and tended to be higher (max. 1.56) in surface snow collected near Ny-Ålesund than at other sites.

### 3.1. April 2016 survey

The spatial variations of $C_{snow}^{EC}$ and $C_{snow}^{OC}$ across the glacier sites surveyed in April 2016 are summarized on **Fig. 3** and **4**, with additional details from snowpits shown in **Fig. S4** and **S5**. In the seasonal snowpack (*n* = 22 sites), $C_{snow}^{EC}$ ranged from <1.0 to 45.2 ng g$^{-1}$, with $\tilde{C}_{snow}^{EC}$ = 2.0 ng g$^{-1}$, while $C_{snow}^{OC}$ ranged from 11.9 to 901.4 ng g$^{-1}$, with $\tilde{C}_{snow}^{OC}$= 48.6 ng g$^{-1}$. These values fall well within the range of $C_{snow}^{EC}$ and $C_{snow}^{OC}$ observed in surface layers on Austre Brøggerbreen between 2007 and 2018 (see also section 3.2). At nearly all of the snowpit sites surveyed in 2016, the $C_{snow}^{EC}$ in surface layers (top 5–10 cm) was larger than the weighted mean for the whole snowpack (**Fig. S6**). This was not the case for $C_{snow}^{OC}$, which showed no systematic enrichment in surface layers relative to the bulk of the snowpack. In the April 2016 snowpack, $C_{snow}^{EC}$ >10 ng g$^{-1}$ were only found on Hansbreen and Werenskioldbreen on southern Spitsbergen (max. 33.0 ng g$^{-1}$). However, comparable $C_{snow}^{EC}$ were measured in surface layers of Kongsvegen and Midtre Lovénbreen, northeastern Spitsbergen, in 2017 (max. 25.4 ng g$^{-1}$), and on Lomonosovfonna, central Spitsbergen, in 2008 (Forsström et al., 2013; interquartile range: 7.3–20.5 ng g$^{-1}$). The snowpack on Hansbreen and Werenskioldbreen also contained the most layers with $C_{snow}^{OC}$ >100 ng g$^{-1}$.

No meaningful differences in $\tilde{C}_{snow}^{EC}$ were found in the April 2016 snowpack across different sectors of Spitsbergen (**Fig. 3**, range: 1.1–2.4 ng g$^{-1}$; Kruskal-Wallis test, $p$ >0.1). However the snowpack on Austfonna (Nordaustlandet) had a significantly lower $\tilde{C}_{snow}^{EC}$ (1.1 ng g$^{-1}$) than on glaciers of southern or northwestern Spitsbergen. This held true even if values of $C_{snow}^{EC}$ <1 ng g$^{-1}$ were excluded. The $C_{snow}^{OC}$ in April 2016 were generally lowest on Lomonosovfonna (central Spitsbergen) and on Austfonna, and highest on southern Spitsbergen glaciers (Hansbreen and Werenskioldbreen). Binning the 2016 snowpit data by elevation (**Fig. 4**) showed no meaningful differences in $\tilde{C}_{snow}^{EC}$ (2.2–2.8 ng g$^{-1}$) or $\tilde{C}_{snow}^{OC}$ (50.3–103.0 ng g$^{-1}$) over the

https://doi.org/10.5194/acp-2020-491
Preprint. Discussion started: 16 June 2020

Atmospheric Chemistry and Physics
Discussions

~1100 m altitude range of the 22 glacier sampling sites (Kruskal-Wallis test, $p$ >0.1). The calculated $L_{snow}^{EC}$ were between 0.1 and 16.2 mg m$^{-2}$ with a median of 0.8 mg m$^{-2}$ (mean 2.0 mg m$^{-2}$), while $L_{snow}^{OC}$ were between 1.7 and 320.1 mg m$^{-2}$, with a median of 20.5 mg m$^{-2}$ (mean 49.3 mg m$^{-2}$). The median EC/OC was only marginally higher (0.06) at glacier sites <200 m a.s.l., compared to higher elevations (range: 0.03–0.04) (**Fig. S7**). As with $\tilde{C}_{snow}^{EC}$ and $\tilde{C}_{snow}^{OC}$, there were no discernible patterns of variation of $L_{snow}^{EC}$ or $L_{snow}^{OC}$ with respect to geographic location (**Fig. S8 and S9**). On most glaciers, $L_{snow}^{EC}$ and/or $L_{snow}^{OC}$ increased with elevation along with $h_{SWE}$. This was most noticeable on Kongsvegen (northwestern Spitsbergen; highest sampling site at 672 m a.s.l.) for both $L_{snow}^{EC}$ or $L_{snow}^{OC}$.

### 3.2. Surface snow monitoring, Brøgger Peninsula

Variations of $C_{snow}^{EC}$, $C_{snow}^{OC}$ and EC/OC measured in the surface snow of central Brøgger Peninsula between 2007 and 2018 are shown on **Fig. 5.** In most months, $C_{snow}^{EC}$ was between 1 and 100 ng g$^{-1}$, and $C_{snow}^{OC}$ between 10 and 1000 ng g$^{-1}$. For years in which snow samples from both areas were obtained, the range of variations on Austre Brøggerbreen ($C_{snow}^{EC}$: <1–45.1 ng g$^{-1}$; $C_{snow}^{OC}$: <1–1076.1 ng g$^{-1}$) overlapped with that near Ny-Ålesund ($C_{snow}^{EC}$: <1–266.5 ng g$^{-1}$; $C_{snow}^{OC}$: <1–7250.3 ng g$^{-1}$; 2 outliers excluded; **Fig. 5a,b**). However on average (all years and months considered), $\tilde{C}_{snow}^{EC}$ near Ny-Ålesund was 3 times higher than on Austre Brøggerbreen, while $\tilde{C}_{snow}^{OC}$ was 7 times higher, but as much as 30 times higher in 2016. There were significant interannual variations in springtime $\tilde{C}_{snow}^{EC}$ (range: 0.4–8.2 ng g$^{-1}$) and $\tilde{C}_{snow}^{OC}$ (range: 1.8–691.4 ng g$^{-1}$) between 2007 and 2018 (**Fig. 5c**). These variations were evident near Ny-Ålesund as well as on Austre Brøggerbreen, which are separated by ~5.5 km and ~400 m in elevation. The highest $\tilde{C}_{snow}^{EC}$ and $\tilde{C}_{snow}^{OC}$ occured in the spring of 2017, and the lowest in the spring of 2014. Depending on site, $\tilde{C}_{snow}^{EC}$ in 2017 was 23 to 27 times higher than in 2014, and $\tilde{C}_{snow}^{OC}$ was 146 to 217 times higher, the largest differences being observed in the snow near Ny-Ålesund. The EC/OC in surface snow varied between 0.01 and 0.42, and variations in springtime EC/OC on Austre Brøggerbreen (2007–18 median: 0.08) generally tracked those at Ny-Ålesund (2010–18 median: 0.10) (**Fig. 5d**). However, variations in $\tilde{C}_{snow}^{EC}$ or EC/OC between 2007 and 2018 did not correlate with those in the median $C_{air}^{eBC}$ measured at Zeppelin Observatory, or with regional monthly snowfall anomalies (**Fig. 5e,f**).

## 4 Discussion

### 4.1. EC and OC in the winter 2015–16 snowpack across Svalbard

The April 2016 survey showed no discernible zonal or latitudinal gradient of $C_{snow}^{EC}$ or $C_{snow}^{EC}$ across Svalbard. As noted earlier, only on Austfonna was $\tilde{C}_{snow}^{EC}$ significantly lower than in some sectors of Spitsbergen. This contrasts with findings from surveys made in the springs of 2007–09, in which $\tilde{C}_{snow}^{EC}$ on Austfonna snow was either comparable to, or larger than, that in central or northeastern Spitsbergen (Forsström et al., 2009, 2013). Based on data from sites where direct comparisons with the 2007–09 surveys are possible, $\tilde{C}_{snow}^{EC}$ in the seasonal snowpack varies, from year to year, by at least one order of magnitude, and sometimes more (**Fig. 3**). The snowpack on glacier sites that are highest and/or further inland (e.g., Lomonosovfonna

https://doi.org/10.5194/acp-2020-491
Preprint. Discussion started: 16 June 2020




summit) had generally lower $C_{snow}^{OC}$ than at low-elevation, near-coastal sites. Ice-free open water areas or frost flowers on sea ice are potential sources of particulate OC aerosols (e.g., microbes, diatoms, plankton, exopolymers from biofilms) during autumn and winter, some of which are likely deposited in snow by settling or through ice nucleation (Bowman and Deming, 2010; Campbell et al., 2018; Karl et al., 2019). The quantity of these aerosols deposited in Svalbard snow might be expected to decrease with inland distance and altitude, which is consistent with our observations of $C_{snow}^{OC}$.

Comparing results of the April 2016 survey with the 2007–09 data from Forsström et al. (2013) also shows that, on an interannual basis, the $L_{snow}^{EC}$ in the late winter snowpack across Svalbard can vary by at least two orders of magnitude (**Fig. S8 and S9**). For the winter 2015–16, our estimates of $L_{snow}^{EC}$ were generally lower than in 2007–09. For example, $L_{snow}^{EC}$ at the summit of Holtedahlfonna (site HDF3; elev. 1119 m a.s.l.) was 1.1 mg m$^{-2}$ in April 2016, which is 70% lower than the 3.7 mg m$^{-2}$ calculated in April 2008 at the same location (Forsström et al., 2013). For their part, Ruppel et al. (2017) estimated an annual mean $L_{snow}^{EC}$ of 10 mg m$^{-2}$ using snow samples and a firn core from Holtedahlfonna spanning ~8 years (2006–14). The corresponding mean $L_{snow}^{EC}$ in the late winter (end April) snowpack could be less than half of this value (~5 mg m$^{-2}$), but the high interannual variability in net snow accumulation at this site (Pramanik et al., 2014; Van Pelt and Kohler, 2015), and the uncertainty in the chronology of the firn core makes such an estimate tentative at best. Differences between our estimates of $L_{snow}^{EC}$ and those from the 2007–09 surveys probably reflect, to a large extent, the variability of atmospheric EC transport and deposition between years and seasons, but also in space (local scale; Svensson et al., 2013).

The estimated $L_{snow}^{EC}$ and $L_{snow}^{OC}$ in the April 2016 snowpack were generally largest at higher elevations on glaciers, where snow accumulation is greater (**Fig. S8 and S9**). From equations (1) and (2) above, it is expected that $L_{snow}^{EC}$ and $L_{snow}^{OC}$ should increase non-linearly with $h_{\mathrm{SWE}}$, since the mass of EC in OC in the snowpack is the cumulative sum of the product of $C_{snow}^{EC}$ (or $C_{snow}^{OC}$) by some fraction of $h_{\mathrm{SWE}}$ in discrete snow layers. For the winter 2015–16 snowpack, we modelled the relationship between $L_{snow}^{EC}$ and $h_{\mathrm{SWE}}$ across all snowpits with an exponential function (**Fig. 6a**; $R^2 = 0.86$; RMSE = 0.59). The goodness-of-fit was confirmed through a Kolmogorov-Smirnov (KS) test of normality on the standardized model residuals ($\alpha = 0.05$, $p = 0.2$). A similar model applied to $L_{snow}^{OC}$ against $h_{\mathrm{SWE}}$ gave a poorer fit (**Fig. 6b**; $R^2 = 0.73$; RMSE = 7.26; KS test: $p = 0.32$), owing to greater scatter in the $L_{snow}^{OC}$ data. The $L_{snow}^{EC}$ estimated by Forsström et al. (2009, 2013) from glacier surveys in 2007–09 showed a much poorer correlation with $h_{\mathrm{SWE}}$ than the April 2016 estimates (**Fig. 6a**). This may partly reflect methodological differences in the estimation of both $L_{snow}^{EC}$ and $h_{\mathrm{SWE}}$ between these studies, and the fact that the estimates from Forsström et al. (2009, 2013) span three different months, whereas the 2016 estimates are based on measurements over a limited time period of ~3 weeks in April.

From the intercept of our exponential model for $L_{snow}^{EC}$, we estimated that the contribution of dry deposition to $L_{snow}^{EC}$ to the winter 2015-16 EC mass accumulation in the glacier snowpits to be ~0.18 mg m$^{-2}$. This represents >50 % of $L_{snow}^{EC}$ at windswept glacier sites with low snow accumulation, but <5 % of $L_{snow}^{EC}$ at sites with $h_{\mathrm{SWE}}$ >1000 mm, such as Hansbreen and Werenskioldbreen in southern Spitsbergen. At the summit of Kongsvegen (site KVG3, elev. 672 m a.s.l.; $h_{\mathrm{SWE}}$ = 825 mm) the estimated dry-deposited EC accounted for only ~11 % of $L_{snow}^{EC}$. This is much less than the ~50 % estimated by Jacobi et al.

https://doi.org/10.5194/acp-2020-491
Preprint. Discussion started: 16 June 2020

Atmospheric Chemistry and Physics
Discussions

(2019) at the same site in March 2012 ($h_{\mathrm{SWE}}$ = 943 mm) using calculations of wet and dry deposition fluxes constrained by refractory black carbon (rBC) measurements in melted snow (SP2 method; Stephens et al., 2003). Our calculated $L_{snow}^{EC}$ for sites with low $h_{\mathrm{SWE}}$, such as those on the lower reaches of glaciers exposed to wintertime katabatic winds, likely underestimate both dry- and wet-deposited EC owing to wind scouring of the snowpack. Nevertheless, our results suggest that the contribution of wintertime dry deposition to $L_{snow}^{EC}$ on Svalbard is likely minor, consistent with findings from recent springtime observations of BC deposition near Ny-Ålesund (Sihna et al., 2018). The estimated monthly mean EC accumulation rates (by wet and dry deposition) at Kongsvegen summit (672 m a.s.l.) and at site ALB2 on Austre Lovénbreen (**Table S1**; 340 m a.s.l.) for the winter 2015–16 were ~0.3 and ~0.1 mg EC m$^{-2}$ mo$^{-1}$, respectively, which are close to those reported by Jacobi et al. (2019) at these two sites for the winter 2011–12 (average: ~0.1–0.2 mg EC m$^{-2}$ mo$^{-1}$).

We applied the exponential models for $L_{snow}^{EC}$ and $L_{snow}^{OC}$ from **Fig. 6** to a map of late winter (30 April) $h_{\mathrm{SWE}}$ generated with the snowpack model in order to project the geographic pattern of EC and OC accumulation across the whole of Svalbard for the winter 2015–16 (**Fig. 7**). The $h_{\mathrm{SWE}}$ data used for this purpose were extracted from the output presented in Van Pelt et al. (2019). Summing the predicted values for $L_{snow}^{EC}$ and $L_{snow}^{OC}$ across the land grid provides estimates of the total aerosol mass that accumulated in the snowpack. The area-averaged loads were 1.8 mg EC m$^{-2}$ and 71.5 mg OC m$^{-2}$. These figures translate to monthly mean accumulation rates of ~0.2 mg EC m$^{-2}$ mo$^{-1}$, and ~8.2 mg OC m$^{-2}$ mo$^{-1}$, respectively, over the period of snow accumulation from 1 Sept. 2015 and 30 April 2016. Averaged on a daily basis, the wintertime EC accumulation rate were ≤0.01 mg EC m$^{-2}$ d$^{-1}$, at the low end of the range of estimated wintertime wet deposition rates for BC aerosols in rural sites elsewhere (~0.1–0.2 mg EC m$^{-2}$ d$^{-1}$; Barrett et al., 2019).

Using the snowpack model, we also estimated the relative contributions to $L_{snow}^{EC}$ and $L_{snow}^{OC}$ made by each of the snowpack layers sampled in the accumulation zone of the 7 glaciers surveyed in April 2016. The number of layers sampled varied from 4 on Austre Lovénbreen and Lomonosovfonna, to 8 on Werenskioldbreen. On-site surface height soundings by AWSs at several glaciers (**Fig. S10**) indicate that snow accumulation in the 2015–16 winter was more or less equally divided between the autumn period leading to the late December 2015 snowstorm, and the months that followed up to mid-/late April 2016, when the snowpits were sampled. The snowpack model simulations, forced with downscaled HIRLAM precipitation data, gave similar results (**Fig. 8**). The AWSs also show that the December 2015 storm saw winter temperatures on nearly all glaciers rise above 0°C for several days, the warming being largest in southern Spitsbergen. Clear evidence for this was found in a >0.2 m thick icy snow layer at mid-depth in the snowpack on Hansbreen (site HB3). The depth of the layer is in good agreement with that predicted by the snowpack model at this site, showing that the simulation provides a reasonable estimate of local surface conditions. Icy layers also occurred in the lower half of the seasonal snowpack on other glaciers, but none of these could be unambiguously ascribed to the late December 2015 storm period.

The timing of EC and OC accumulation, inferred from the snowpack model chronology, varied considerably between glaciers (**Fig. 9**). On Austfonna in Nordaustlandet, ~80 % of the EC and OC was found in snow layers estimated to have been deposited in or after December 2015. On glaciers of northern and central Spitsbergen (Austre Lovénbreen, Kongsvegen, Holtedahlfonna and Lomonosovfonna), the accumulation sequence was more variable and differed between EC and OC. On

https://doi.org/10.5194/acp-2020-491
Preprint. Discussion started: 16 June 2020

Atmospheric Chemistry and Physics
Discussions

Hansbreen and Werenskioldbreen in southern Spitsbergen, most of the EC and OC was contained in the deeper layers of the seasonal snowpack, estimated to have been deposited prior to January 2016. Surface meteorological records from the Polish Polar Station Hornsund and from an AWS on Werenskioldbreen show that several large snowfall events occurred in this area during the autumn of 2015, as well as some thaw events (**Fig. S10**). The stratigraphy of snowpits excavated on Hansbreen and Werenskioldbreen in April 2016 also showed clear evidence of melt-freeze events in the early part of the 2015–16 winter (e.g., site HB3 on Hansbreen; **Fig. 8**). Also visible in these snowpits were multiple positive excursions in $\delta^{18}O$ (i.e. shifts to less negative values) indicative of snowfall events presumably associated with relatively moist and warm southerly air intrusions over Spitsbergen.

Large cyclonic storms that reach Svalbard in December typically track from the south-southeast (Rinke et al., 2017), and often make their landfall on southern Spitsbergen, bringing heavy snowfall and relatively warm, moist air, as for example on 19 December 2015 (Hancock et al., 2018). Such events may enhance wet deposition of EC and OC aerosols on local glaciers such as Hansbreen and Werenskioldbreen, relative to more northerly sectors of Spitsbergen that are located further along the storm track. Previous observations of acidic snowfall deposition on Hansbreen during periods of southerly polluted air advection support this interpretation (Nawrot et al., 2016). Furthermore, meltwater percolation during surface thaws (or rain-on-snow) can redistribute or concentrate some of the more hydrophilic EC and OC into icy layers near the base of the snowpack (Aamaas et al., 2011; Xu et al., 2012). These circumstances could explain why the $L_{snow}^{EC}$ and $L_{snow}^{OC}$ were particularly high in the accumulation zones of Hansbreen and Werenskioldbreen in April 2016, and also why >65 % of the accumulated EC was found in the deepest part of the snowpack at these sites. It also suggests that a few large precipitation events could explain a large part of the interannual variability in $L_{snow}^{EC}$ and $L_{snow}^{OC}$ across Svalbard, as was previously observed for wet deposition of $SO_4^{2-}$, $NO_3^-$ and OC on glaciers near Hornsund (Kühnel et al., 2013; Kozioł et al., 2019).

### 4.2. EC and OC in surface snow, Brøgger Peninsula.

Two features of the ~11-year record of $C_{snow}^{EC}$ and $C_{snow}^{OC}$ from Brøgger Peninsula (**Fig. 5**) are of particular interest: the difference in $\tilde{C}_{snow}^{EC}$ and $\tilde{C}_{snow}^{OC}$ between Ny-Ålesund and Austre Brøggerbreen, and the synchronous interannual variations at both sites. The generally higher $\tilde{C}_{snow}^{EC}$ and $\tilde{C}_{snow}^{OC}$ near Ny-Ålesund compared to Austre Brøggerbreen point to the probable existence of a wintertime gradient in atmospheric EC and OC deposition from sea level up to at least 456 m a.s.l. on this part of Brøgger Peninsula. Evidence for such a gradient was observed during experimental snowmobile-based surveys of near-surface $C_{air}^{eBC}$ over Edithbreen and Kongsvegen (see **Fig. 1** and **S2** for locations) made in April 2016 (Spolaor et al., 2017). Such a situation may not, however, necessarily persist in all winter months. For example, Aamaas et al. (2011) measured a $\tilde{C}_{snow}^{EC}$ of 6.6 ng $g^{-1}$ near Ny-Ålesund in March 2008, which was very close to the mean of 6.3 ng $g^{-1}$ on Austre Brøggerbreen snow during the same month. Variations in the frequency and strength of near-surface thermal inversions could account for fluctuations in $C_{snow}^{EC}$ and $C_{snow}^{OC}$ gradients between the coast and the accumulation area of Austre Brøggerbreen, as was shown to be the case for atmospheric $SO_4^{2-}$ aerosols (Dekhtyareva et al., 2018). Stable inversion layers established by strong surface

https://doi.org/10.5194/acp-2020-491
Preprint. Discussion started: 16 June 2020

Atmospheric Chemistry and Physics
Discussions

radiative cooling could trap aerosols emitted from Ny-Ålesund (EC) or from nearby open waters or sea ice (OC), leading to enhanced concentrations of these aerosols in coastal surface snow during these periods. Aamaas et al. (2011) could not detect local EC pollution in coastal snow within 20 km of Ny-Ålesund, but as these authors pointed out, this could have been due to unfavourable wind conditions at the time of their sampling. Our data, however, suggest that that winter/spring surface snow near Ny-Ålesund is commonly enriched in EC relative to OC when compared to snow deposited higher up on Austre Brøggerbreen, as shown by ~4-fold differences in the median EC/OC between these sites (**Table 2**).

The median EC/OC in snow at Ny-Ålesund and Austre Brøggerbreen was <0.10 prior to 2010, but rose to 0.43 and 0.20, respectively, in 2015, and declined after 2016. The seasons with highest median EC/OC (2013–15) were also those with lowest $\tilde{C}_{snow}^{EC}$ and $\tilde{C}_{snow}^{OC}$, which implies that meteorological and/or other conditions must have prevailed which limited atmospheric deposition of OC and EC in snow, OC being more affected than EC. Possible causal factors include sea ice cover or sea-surface winds, which partly modulate emissions of marine organic aerosol (e.g., Kirpes et al., 2019), or katabatic winds from Kongsfjorden, that can affect the thermal stratification of boundary layer air in winter months (Esau and Repina, 2012; Maturilli and Kayser, 2017).

Between 2008 and 2018 (the years in which snow sampling was most thorough), $\tilde{C}_{snow}^{EC}$ on Brøgger Peninsula varied by up to 35 ng g$^{-1}$, and $\tilde{C}_{snow}^{OC}$ by up to 689 ng g$^{-1}$. However, there were no significant trends in either $\tilde{C}_{snow}^{EC}$ or $\tilde{C}_{snow}^{OC}$ over the whole period (Mann-Kendall test; $p >> 0.05$). Data from the April 2016 glacier survey (**Fig. 6**), as well as previous studies (Bourgeois and Bey, 2011; Browse et al., 2012) suggest that wet deposition is the predominant mode of EC deposition in Arctic snow. To control for the possible role of snowfall rate, we compared $\tilde{C}_{snow}^{EC}$ in surface layers for March, April and May (MAM) 2008–18 with simulated monthly snowfall anomalies over central Brøgger Peninsula over the same period. However, as mentioned earlier, no significant correlation was found, (**Fig. 5f**).

A simple metric used to quantify wintertime wet deposition of BC is the snow washout ratio $W$ (sometimes called scavenging ratio), and defined as $C_{snow}^{BC}/C_{air}^{BC}$, which accounts for atmospheric BC removal by snowfall through both within- and below-cloud nucleation scavenging (Noone and Clark, 1988). Previous observations made during springtime snowfall events on Svalbard have yielded a wide range of estimates for $W$ of ~13 to 2000, with a median of ~380 at Zeppelin Observatory, and of ~60 to 600 in Ny-Ålesund (Hegg et al., 2011; Gogoi et al., 2018). Here, we used our data on $C_{snow}^{EC}$ in spring snow at Austre Brøggerbreen, combined with $C_{air}^{eBC}$ measured at Zeppelin Observatory, to constrain plausible estimates of $W$ (**Fig. 10**). Specifically, we compared the probability distribution of $C_{snow}^{EC}$ in surface layers at Austre Brøggerbreen with that calculated from $C_{air}^{BC}$ at Zeppelin Observatory during the same time periods, in order to identify values of $W$ that produced an optimal match. The calculation was:

$$\bar{C}_{snow}^{eBC} = \frac{W \times \sum_{i=1}^{t} \left( \frac{C_{air}^{eBC} \times f}{\rho_{air}} \right)_i}{t} \quad (4)$$

https://doi.org/10.5194/acp-2020-491
Preprint. Discussion started: 16 June 2020

Atmospheric Chemistry and Physics
Discussions

where $\bar{C}_{snow}^{eBC}$ is the estimated mean concentration of eBC in the top 5 cm of the snowpack for the dates on which snow samples were actually obtained, *t* is the number of days prior to the snow sampling date over which the computed values of $C_{snow}^{eBC}$ were averaged, *W* is the washout ratio, $\rho_{air}$ the air density and *f* is a precipitation weighing factor. We performed this calculation for 54 snow sampling days during the spring months of 2011–18, which are the months (years) in which the $C_{air}^{eBC}$ data had the fewest missing values. The simulated snowpack at Austre Brøggerbreen summit was used to estimate, for each day, the value of *t* (averaging interval) based on prior changes in the snow surface height. This varied between 3 and 24 days. The weighing factor *f* was calculated from changes in $h_{SWE}$ for days on which the simulated snowpack surface rose by ≥ 1 mm (i.e., on days without snowfall, *f* was 0). Monthly mean values of $\rho_{air}$ were used, calculated from Ny-Ålesund radiosonde data (Maturilli, 2011 and seq.).

An overlap between the calculated $\bar{C}_{snow}^{eBC}$ and measured $C_{snow}^{EC}$ was obtained for $10 \leq W \leq 300$ (**Fig. 10**). These values agree well with those reported by Gogoi et al. (2018) for Ny-Ålesund (~13–270), but are low compared to those of Hegg et al. (2011) for Zeppelin Observatory (~250–2000). There are, however, several sources of uncertainty in the calculated $\bar{C}_{snow}^{eBC}$. First, the calculation uses $C_{air}^{eBC}$ measured at Zeppelin Observatory (474 m a.s.l.), whereas aerosols are likely scavenged by snowfall over a range of altitudes with variable BC mixing ratios. Second, the calculation neglects dry deposition contributions. Third, the simulated snow surface changes at Austre Brøggerbreen that were used to define the averaging period *t* for $C_{air}^{eBC}$ do not account for the possible effect of snow drifting and mixing. Consequently, the comparison presented on **Fig. 10** should be considered with some caution. What the results imply is simply that it is possible to forecast a realistic range of eBC (or EC) concentrations in surface snow at Austre Brøggerbreen using $C_{air}^{eBC}$ at Zeppelin Observatory and *W* values of 10 to 300.

### 4.3. Placing results in geographic perspective

**Figure 11** shows the range of $C_{snow}^{EC}$ in winter/spring Svalbard snow measured in this study, compared with data from other circum-Arctic or subarctic sites sampled between 2002 and 2018 (see figure caption for data sources). All EC data in this comparison were obtained by thermo-optical measurements on snow filters, but variations in the thermal protocol used between studies may account for some of the inter-site differences (**Table S4**). The $C_{snow}^{EC}$ measurements made by Aamas et al. (2011) near Longyearbyen were excluded because of local pollution of the snow cover by coal dust (Khan et al., 2017). The pattern of EC distribution in winter/spring snow across the circum-Arctic shows the lowest $\tilde{C}_{snow}^{EC}$ in central Greenland (<1 ng g$^{-1}$), followed by the southwestern Yukon (3–5 ng g$^{-1}$), northern and central Alaska (3–5 ng g$^{-1}$), Svalbard (2–7 ng g$^{-1}$ outside Ny-Ålesund), northern Scandinavia (~15–30 ng g$^{-1}$ depending on site), and reaching maximum values of $\tilde{C}_{snow}^{EC}$ in eastern and central Siberia (35–66 ng g$^{-1}$). This geographic pattern is in broad agreement with that observed in pan-Arctic surveys conducted in 2007–09 (Doherty et al., 2010) and between 2012 and 2016 (Mori et al., 2019) using other analytical methods. The EC/OC (inset, **Fig. 11**) in the Svalbard snowpack outside Ny-Ålesund averages 0.07±0.08 (1 s.d.), which is similar, within

https://doi.org/10.5194/acp-2020-491
Preprint. Discussion started: 16 June 2020

Atmospheric Chemistry and Physics Discussions

errors, to that reported in snowpacks in central Greenland (0.08±0.05; Hagler et al*.*, 2007), northern Alaska (0.09±0.03; Dou et al., 2017), northeastern Russia and Siberia (0.07±0.03; Evangeliou et al., 2018), and northern Finland (0.05±0.06; Meinander et al., 2013). The only site where a significantly lower mean EC/OC in snow has been measured is on the Eclipse Icefield in the southern Yukon (0.01±0.01; **Table S5**). This may be explained by the remoteness of this high elevation site (3020 m a.s.l.), which is mostly exposed in winter to relatively clean air advected from the Gulf Alaska.

## 5 Summary and conclusions

We have presented a large dataset of observations of atmospheric EC and OC deposited in snow on the archipelago of Svalbard, made between 2007 and 2018. The spatial snow survey conducted across 22 glacier sites in April 2016 was one of the most extensive and detailed carried out on Svalbard, and allows direct comparisons with the surveys by Forsström et al. (2009, 2013), made nearly 10 years earlier. Across all glacier sites, $C_{snow}^{EC}$ in the snowpack ranged from <1.0 to 45.2 ng g$^{-1}$ (median 2.0 ng g$^{-1}$), while $C_{snow}^{OC}$ ranged from 11.9 to 3448.9 ng g$^{-1}$ (median 48.6 ng g$^{-1}$). The calculated $L_{snow}^{\mathrm{EC}}$ were between 0.1 and 16.2 mg m$^{-2}$ (median 0.8 mg m$^{-2}$), while $L_{snow}^{OC}$ were between 1.7 and 320.1 mg m$^{-2}$ (median 20.5 mg m$^{-2}$). The $\tilde{C}_{snow}^{EC}$ and $L_{snow}^{EC}$ in 2016 were comparable or lower than those found in spring 2007–09 glacier snow, but no clear spatial gradients could be identified across the archipelago. Both $L_{snow}^{EC}$ and $L_{snow}^{OC}$ were found to increase exponentially with elevation and $h_{\mathrm{SWE}}$. Using these relationships, we estimated the area-averaged, monthly mean EC and OC accumulation rates over the whole of Svalbard to be ~0.2 mg EC m$^{-2}$ mo$^{-1}$ and ~8.9 mg OC m$^{-2}$ mo$^{-1}$ for the winter 2015–16 (September to April). The relationship between $L_{snow}^{EC}$ and $h_{\mathrm{SWE}}$ also point to dry EC deposition in snow being minor compared to wet deposition. The accumulation of EC and OC in the snowpack was inferred to be equally distributed over the winter 2015–16 at most sites. Relatively high $L_{snow}^{EC}$ and $L_{snow}^{OC}$ were found in the accumulation zones of glaciers on southern Spitsbergen, which we attribute to enhanced wet aerosol deposition when large Atlantic cyclonic storms made landfall in this area during the autumn and mid-winter.

The set of EC and OC measurements made in surface snow on Brøgger Peninsula in 2007–18 is one of the longest such datasets available from the Arctic. During this period, the range of $C_{snow}^{EC}$ and $C_{snow}^{OC}$ near Ny-Ålesund (50 m a.s.l.) overlapped with that at Austre Brøggerbreen (456 m a.s.l.). However, $\tilde{C}_{snow}^{EC}$ near Ny-Ålesund was, on average, 3 times higher than on Austre Brøggerbreen, while $\tilde{C}_{snow}^{OC}$ was 7 times higher, pointing to an elevation gradient in EC and OC deposition between these sites. While no long-term trends were detected over the period 2007–18, $\tilde{C}_{snow}^{EC}$ and $\tilde{C}_{snow}^{OC}$ showed synchronous interannual variations between the snow sampling sites, the largest ones occurring near Ny-Ålesund. The EC/OC in snow also showed interannual variations with large differences between Ny-Ålesund and Austre Brøggerbreen, which are likely controlled by changes in the frequency and strength of wintertime near-surface thermal inversions in the area. Further investigations of winter/spring micro- to mesoscale meteorological conditions are needed to clarify what these variations might imply about the dynamics of atmospheric EC and OC deposition in snow at these sites. We used the measured $C_{snow}^{EC}$ on Austre Brøggerbreen summit combined with $C_{air}^{eBC}$ data from Zeppelin Observatory and snow modelling to constrain plausible

Atmospheric Chemistry and Physics
Discussions

estimates of the snowfall washout ratio $W$ for EC, and found that values of 10 to 300 produce a realistic range of $C_{snow}^{eBC}$ in spring surface snow. Extending the surface snow monitoring program for EC and OC on Austre Brøggerbreen would allow to test the robustness of these findings. Finally, comparing results from this study to those from other surveys confirms the existence of a broad longitudinal gradient in EC deposition across the Arctic and sub-Arctic, with the lowest $\tilde{C}_{snow}^{EC}$ found in the western Arctic (Alaska, Yukon) and central Greenland, and the highest in northwestern Russia and Siberia.

*Data availability.*

The data presented in this article can be downloaded from Pangea *[Dataset submitted on 19 May 2020, submission tracker # PDI-24118, doi pending]*.

*Author contributions.*

JCG, MB, CL, BL, TS, CZ and others initiated the April 2016 survey. JCG oversaw the snow sampling program on Brøgger Peninsula. UL and JC performed the EC and OC analyses, and TM the $\delta^{18}O$ analyses. WvP carried out the snow model simulations. CZ wrote the manuscript, with contributions from all co-authors.

*Competing interests.*

The authors declare that they have no conflict of interest.

*Acknowledgements.*

The April 2016 survey on Svalbard was funded through a grant from the Svalbard Science Forum (RIS 10472) to J.-C. Gallet and others, and surface snow monitoring on Brøgger Peninsula was conducted by the Norwegian Polar Institute (NPI) with support from Svalbardmiljøfonds and from the Swedish Research Council Formas project "Black and White" (grant 2006-00210 to J. Ström and others). Logistical support for field work in 2016 was provided by NPI, the University of Oslo, the Swedish Research Council and the Swedish Polar Secretariat, the Ice and Climate and the Environment research group at Uppsala University, the Institute of Geophysics of the Polish Academy of Sciences (PAS), the Centre for Polar Studies at the University of Silesia (USi), the Polish Ministry of Science and Higher Education (statutory activities 3841/E-41/S/2020), and the Institut Paul-Emile Victor (France). A. Uszczyk (USi), D. Ignatiuk (Svalbard Integrated Arctic Earth Observing System), M. Grabiec and D. Kępski (PAS) participated in the snow sampling work near Horsund. Planning and collaborative work between the study co-authors was facilitated by funds from the Swedish Strategic Research Area initiative "Biodiversity and Ecosystem services in a Changing Climate" through Gothenburg University, the Gothenburg Air and Climate Network and the International Arctic Science Committee.

https://doi.org/10.5194/acp-2020-491
Preprint. Discussion started: 16 June 2020




**References**

Aamaas, B., Bøggild, C.E., Stordal, F., Berntsen, T., Holmén, K. and Ström, J.: Elemental carbon deposition to Svalbard snow from Norwegian settlements and long-range transport, Tellus, 63B, 340–351, doi:10.1111/j.1600-0889.2011.00531.x, 2011.

AMAP: AMAP Assessment 2015: Black carbon and ozone as Arctic climate forcers. Arctic Monitoring and Assessment Programme (AMAP), Oslo, Norway. vii + 116 pp, 2015.

Backman, J., Schmeisser, L., Virkkula, A., Ogren, J. A., Asmi, E., Starkweather, S., Sharma, S., Eleftheriadis, K., Uttal, T., Jefferson, A., Bergin, M., Makshtas, A., Tunved, P., and Fiebig, M.: On Aethalometer measurement uncertainties and an instrument correction factor for the Arctic, Atmos. Meas. Tech., 10, 5039–5062, doi:10.5194/amt-10-5039-2017, 2017.

Barrett, T.E., Ponette-Gonzáleza, A.G., Rindya, J.E., and Weathers, K.C.: Wet deposition of black carbon: A synthesis, Atmos. Environ. 213, 558–567, doi: 10.1016/j.atmosenv.2019.06.033, 2019.

Binder, H., Boettcher, M., Grams, C. M.,Joos, H., Pfahl, S., & Wernli, H.: Exceptional air mass transport and dynamical drivers of an extreme wintertime Arctic warm event. Geophys. Res. Lett., 44, 12,028–12,036, doi:10.1002/2017GL075841, 2017.

Bond, T. C., Doherty, S. J., Fahey, D. W., Forster, P. M., Berntsen, T., DeAngelo, B. J., Flanner, M. G., Ghan, S., Kärcher, B., Koch, D., Kinne, S., Kondo, Y., Quinn, P. K., Sarofim, M. C., Schultz, M. G., Schulz, M., Venkataraman, C., Zhang, H., Zhang, S., Bellouin, N., Guttikunda, S. K., Hopke, P. K., Jacobson, M. Z., Kaiser, J. W., Klimont, Z., Lohmann, U., Schwarz, J. P., Shindell, D., Storelvmo, T., Warren, S. G., and Zender, C. S.: Bounding the role of black carbon in the climate system: A scientific assessment, J. Geophys. Res. Atmos., 118, 5380–5552, doi:10.1002/jgrd.50171, 2013.

Bond, T.C., Anderson, T. L., and Campbell, D.: Calibration and intercomparison of filter-based measurements of visible light absorption by aerosols, Aerosol Sci. Tech. 30, 582–600, doi: 10.1080/027868299304435, 1999.

Bourgeois, Q. and Bey, I.: Pollution transport efficiency toward the Arctic: Sensitivity to aerosol scavenging and source regions, J. Geophys. Res. 116, D08213, doi:10.1029/2010JD015096, 2011.

Bowman, D.S. and Deming, J.W.: Elevated bacterial abundance and exopolymers in saline frost flowers and implications for atmospheric chemistry and microbial dispersal, Geophys. Res. Lett. 37, L13501, doi:10.1029/2010GL043020, 2010.

Browse, J., Carslaw, K. S., Arnold, S. R., Pringle, K., and Boucher, O.: The scavenging processes controlling the seasonal cycle in Arctic sulphate and black carbon aerosol, Atmos. Chem. Phys., 12, 6775–6798, doi:10.5194/acp-12-6775-2012, 2012.

Campbell, K., Muncy, C.J., Belzile, C., Delaforge, A. and Rysgaard, S.: Seasonal dynamics of algal and bacterial communities in Arctic sea ice under variable snow cover, Polar Biol., 41, 41–58, doi:10.1007/s00300-017-2168-2,

https://doi.org/10.5194/acp-2020-491
Preprint. Discussion started: 16 June 2020



2018.

Cavalli, F., Viana, M., Yttri, K. E., Genberg, J., and Putaud, J.-P.: Toward a standardised thermal-optical protocol for measuring atmospheric organic and elemental carbon: the EUSAAR protocol, Atmos. Meas. Tech., 3, 79–89, doi:10.5194/amt-3-79-2010, 2010.

Cheng, Y., Hea, K.-B., Duana, F.-K., Du, Z.-L., Zheng, M. and Ma, Y.-L.: Ambient organic carbon to elemental carbon ratios: Influence of the thermal–optical temperature protocol and implications, Sci. Tot. Environ., 468–469, 1103–1111, doi:10.1016/j.scitotenv.2013.08.084, 2014.

Chow, J. C., Watson, J. G., Chen, L. W. A., Arnott, W. P., Moosmüller, H., and Fung, K.: Equivalence of elemental carbon by thermal/optical reflectance and transmittance with different temperature protocols, Environ. Sci. Technol., 38, 4414–4422, doi: 10.1021/es034936u, 2004.

Conger, S.M. and McClung, D.M.: Comparison of density cutters for snow profile observations, J. Glaciol. 55, 189, doi:10.3189/002214309788609038, 2009.

Dee, D.P., Uppala, S.M., Simmons, A.J., Berrisford, P., Poli, P., Kobayashi, S., Andrae, U., Balmaseda, M.A., Balsamo, G., Bauer, P., Bechtold, P., Beljaars, A.C.M., van de Berg, L., Bidlot, J., Bormann, N., Delsol, C., Dragani, R., Fuentes, M., Geer, A.J., Haimberger, L., Healy, S.B., Hersbach, H., Hólm, E.V., Isaksen, L., Kållberg, P., Köhler, M., Matricardi, M., McNally, A.P., Monge-Sanz, B.M., Morcrette, J.-J., Park, B.-K., Peubey, C., de Rosnay, P., Tavolato, C., Thépaut, J.-N. and Vitart, F.: The ERA-Interim reanalysis: configuration and performance of the data assimilation system. *Q. J. R. Meteorol. Soc.*, 137: 553-597, doi:10.1002/qj.828, 2011.

Dekhtyareva, A., Holmén, K., Maturilli, M., Hermansend, O. and Graversen, R.: Effect of seasonal mesoscale and microscale meteorological conditions in Ny-Ålesund on results of monitoring of long-range transported pollution, Polar Res., 37, 1508196, doi: 10.1080/17518369.2018.1508196, 2018.

Doherty, S. J., Warren, S. G., Grenfell, T. C., Clarke, A. D., and Brandt, R. E.: Light-absorbing impurities in Arctic snow, Atmos. Chem. Phys., 10, 11647–11680, doi:10.5194/acp-10-11647-2010, 2010.

Dou, T., Xiao, C., Du, Z., Schauer, J.J., Ren, H., Ge, B., Xie, A., Tan, J., Fu, P. and Zhang, Y.: Sources, evolution and impacts of EC and OC in snow on sea ice: a measurement study in Barrow, Alaska, Sci. Bull. 62, 1547–1554, doi:10.1016/j.scib.2017.10.014, 2017.

Eleftheriadis, K., Vratolis, S. and Nyeki, S.: Aerosol black carbon in the European Arctic: Measurements at Zeppelin station, Ny-Ålesund, Svalbard from 1998–2007, Geophys. Res. Lett., 36, L02809, doi:10.1029/2008GL035741, 2009.

Esau, I. and Repina, I.: Wind climate in Kongsfjorden, Svalbard, and attribution of leading wind driving mechanisms through turbulence-resolving simulations, Adv. Meteorol., 568454, doi: 10.1155/2012/568454, 2012.

Esau, I. and Sorokina, S.: *Climatology of the Arctic planetary boundary layer*, in Peter R. Lang, P.R. and Lombargo, F. S. (Eds.): Atmospheric Turbulence, Meteorological Modeling and Aerodynamics, Nova Science Publishers, pp. 3–58, 2009.

Evangeliou, N., Shevchenko, V. P., Yttri, K. E., Eckhardt, S., Sollum, E., Pokrovsky, O. S., Kobelev, V. O., Korobov, V. B., Lobanov, A. A., Starodymova, D. P., Vorobiev, S. N., Thompson, R. L., and Stohl, A.: Origin of elemental carbon in snow from western Siberia and northwestern European Russia during winter–spring 2014, 2015 and 2016, Atmos. Chem. Phys., 18, 963–977, doi:10.5194/acp-18-963-2018, 2018.

Forsström, S., Isaksson, E., Skeie, R. B., Ström, J., Pedersen, C. A., Hudson, S. R., Berntsen, T. K., Lihavainen, H., Godtliebsen, F. and Gerland, S. : Elemental carbon measurements in European Arctic snow packs, J. Geophys. Res. Atmos., 118, 13,614–13,627, doi:10.1002/2013JD019886, 2013.

Forsström, S., Ström, J., Pedersen, J. C. A., Isaksson, E., and Gerland, S.: Elemental carbon distribution in Svalbard snow, J. Geophys. Res. Atmos. 114, D19112, doi:10.1029/2008JD011480, 2009.

Gallet, J. C., Björkman, M. P., Larose, C., Luks, B., Martma, T., and Zdanowicz, C.: *Protocols and recommendations for the measurement of snow physical properties, and sampling of snow for black carbon, water isotopes, major ions and microorganisms*. Tromsø: Norwegian Polar Institute, Short Report 46, 29 p., 2018.

Ganser, G.H. and Hewett, P.: An accurate substitution method for analyzing censored data, J. Occup. Environ. Hyg., 7, 233–244, doi:10.1080/15459621003609713, 2010.

Gogoi, M.M., Babu, S.S., Pandey, S.K., Nair, V.S., Vaishya, A., Girach, A.I.A. and Koushik, N.: Scavenging ratio of black carbon in the Arctic and the Antarctic, Polar Science, 16, 10–22, doi:10.1016/j.polar.2018.03.002, 2018.

Hagler, G. S. W., Bergin, M.H., Smith, E.A., Dibb, J.E., Anderson, C. and Steig, E.J.: Particulate and water-soluble carbon measured in recent snow at Summit, Greenland, Geophys. Res. Lett., 34, L16505, doi:10.1029/2007GL030110, 2007.

Hancock, H., Prokop, A., Eckerstorfer, M. and Hendrik, J.: Combining high spatial resolution snow mapping and meteorological analyses to improve forecasting of destructive avalanches in Longyearbyen,Svalbard, Cold Reg. Sci. Tech. 154, 120–132, doi:10.1016/j.coldregions.2018.05.011, 2018.

Hegg, D.A., Clarke, A.D., Doherty, S.J. and Ström, J.: Measurements of black carbon aerosol washout ratio on Svalbard, Tellus, 63B, 891–900, doi:10.1111/j.1600-0889.2011.00577.x, 2011.

Hornung, R.W. and Reed, L.D.: Estimation of average concentration in the presence of nondetectable values, *Appl. Occup. Environ. Hyg.*, 5 (1), doi: 10.1080/1047322X.1990.10389587, 1990.

Jacobi, H.-W., Obleitner, F., Da Costa, S., Ginot, P., Eleftheriadis, K., Aas, W. and Zanatta, M.: Deposition of ionic species and black carbon to the Arctic snowpack: combining snow pit observations with modeling, Atmos. Chem. Phys., 19, 10361–10377, doi:10.5194/acp-19-10361-2019, 2019.

James, T. D., Murray, T., Barrand, N. E., Sykes, H. J., Fox, A J., and King, M. A.: Observations of enhanced thinning in the upper reaches of Svalbard glaciers, Cryosphere, 6, 1369–1381, doi:10.5194/tc-6-1369-2012, 2012.

Karl, M., Leck, C., Rad, F.M., Bäcklund, A., Lopez-Aparicio, S. and Heintzenberg, J.: New insights in sources of the sub-micrometre aerosol at Mt. Zeppelin observatory (Spitsbergen) in the year 2015. Tellus B, 71, 1613143, doi:10.1080/16000889.2019.1613143, 2019.

Khan, A. L., Dierssen, H., Schwarz, J. P., Schmitt, C., Chlus, A., Hermanson, M., Painter, T.H. and McKnight, D.M.: Impacts of coal dust from an active mine on the spectral reflectance of Arctic surface snow in Svalbard, Norway, J. Geophys. Res. Atmos., 122, 1767–1778, doi:10.1002/2016JD025757, 2017.

Kim, B., Hong, J., Jun, S. Zhang, X., Kwon, H., Kim, S., Kim, J. and Kim, H.: Major cause of unprecedented Arctic warming in January 2016: Critical role of an Atlantic windstorm, Sci. Rep., 7, 40051, doi:10.1038/srep40051, 2017.

Kirpes, R.M., Bonanno, D., May, N.W., Fraund, M., Barget, A.J., Moffet, R.C., Ault, A.P. and Pratt, K.A.: Wintertime Arctic sea spray aerosol composition controlled by sea ice mead microbiology, ACS Cent. Sci. 5, 11, 1760-1767, doi:10.1021/acscentsci.9b00541, 2019.

Koenig, L. S., Ivanoff, A., Alexander, P. M., MacGregor, J. A., Fettweis, X., Panzer, B., Paden, J. D., Forster, R. R., Das, I., McConnell, J. R., Tedesco, M., Leuschen, C., and Gogineni, P.: Annual Greenland accumulation rates (2009–2012) from airborne snow radar, The Cryosphere, 10, 1739–1752, doi:10.5194/tc-10-1739-2016, 2016.

König, M., Nuth, C., Kohler, J., Moholdt, G., and Pettersson, R.: A digital glacier database for svalbard, in Kargel, J.S., Leonard, G.J., Bishop, M.P., Kääb, A. and Raup, B.H. (Eds.), *Global Land Ice Measurements from Space*, Springer, pp. 229–239, 2014.

Kozioł, K. A., Moggridge, H. L., Cook, J. M. and Hodson, A. J.: Organic carbon fluxes of a glacier surface: A case study of Foxfonna, a small Arctic glacier, *Earth Surf. Processes Landforms* 44 (2), 405–416, doi:10.1002/esp.4501, 2019.

Kühnel, R., Björkman, M.P., Vega, C.P., Hodson, A., Isaksson, E. and Ström, J.: Reactive nitrogen and sulphate wet deposition at Zeppelin Station, Ny-Ålesund, Svalbard, Polar Research 32, 19136, doi:10.3402/polar.v32i0.19136, 2013.

Lim, S., Faïn, X., Zanatta, M., Cozic, J., Jaffrezo, J.-L., Ginot, P., and Laj, P.: Refractory black carbon mass concentrations in snow and ice: method evaluation and inter-comparison with elemental carbon measurement, Atmos. Meas. Tech., 7, 3307–3324, doi:10.5194/amt-7-3307-2014, 2014.

Lis, G., Wassenenaar L. I. and Hendy M. J.: High-precision laser spectroscopy D/H and $^{18}O/^{16}O$ measurements of microliter natural water samples, Anal. Chem. 80, 287–293, doi:10.1021/ac701716q, 2008.

Marchenko S., van Pelt W.J.J., Claremar B., Pohjola V., Pettersson R., Machguth H. and Reijmer C.: Parameterizing deep water percolation improves subsurface temperature simulations by a multilayer firn model, Frontiers in Earth Sciences, 5,16, doi:10.3389/feart.2017.00016, 2017.

Marks, A. A. and King, M. D.: The effects of additional black carbon on the albedo of Arctic sea ice: variation with sea ice type and snow cover, The Cryosphere, 7, 1193–1204, doi:10.5194/tc-7-1193-2013, 2013.

Maturilli, M. and Kayser, M.: Arctic warming, moisture increase and circulation changes observed in the Ny-Ålesund homogenized radiosonde record, Theor. Appl. Climat., 130, 1–2, 1–17, doi:10.1007/s00704-016-1864-0, 2017.

Maturilli, M. Radiosonde measurements from station Ny-Ålesund (2011-01). Alfred Wegener Institute - Research Unit Potsdam, PANGAEA, doi:10.1594/PANGAEA.757557, 2011.

Meinander, O., Kazadzis, S., Arola, A., Riihelä, A., Räisänen, P., Kivi, R., Kontu, A., Kouznetsov, R., Sofiev, M., Svensson, J., Suokanerva, H., Aaltonen, V., Manninen, T., Roujean, J.-L., and Hautecoeur, O.: Spectral albedo of seasonal snow during intensive melt period at Sodankylä, beyond the Arctic Circle, Atmos. Chem. Phys., 13, 3793–3810, doi:10.5194/acp-13-3793-2013, 2013.

Mori, T., Goto-Azuma, K., Kondo, Y., Ogawa-Tsukagawa, Y., Miura, K., Hirabayashi, M., Oshima, N., Koike, M., Kupiainen, K., Moteki, N., Ohata, S., Sinha, P.R., Sugiura, K., Aoki, T., Schneebeli, M., Steffen, K., Sato, A., Tsushima, A., Makarov, V., Omiya, S., Sugimoto, A., Takano, S. and Nagatsuka, N.: Black carbon and inorganic aerosols in Arctic snowpack. J. Geophys. Res. Atmos., 124, 13,325–13,356, doi:10.1029/2019JD030623, 2019.

Nawrot, A.P., Migała, K., Luks, B., Pakszys, P. and Głowacki, P., Chemistry of snow cover and acidic snowfall during a season with a high level of air pollution on the Hans Glacier, Spitsbergen, Polar Sci. 10, 249–261, doi:10.1016/j.polar.2016.06.00, 2016.

Noone, K. J. and Clarke, A. D.: Soot scavenging measurement in Arctic snowfall, Atmos. Environ., 22, 2773–2778, doi: 10.1016/0004-6981(88)90444-1, 1988.

Osmont, D., Wendl, I. A., Schmidely, L., Sigl, M., Vega, C. P., Isaksson, E., and Schwikowski, M.: An 800-year high-resolution black carbon ice core record from Lomonosovfonna, Svalbard, Atmos. Chem. Phys., 18, 12777–12795, doi:10.5194/acp-18-12777-2018, 2018.

Petzold, A., Ogren, J. A., Fiebig, M., Laj, P., Li, S.-M., Baltensperger, U., Holzer-Popp, T., Kinne, S., Pappalardo, G., Sugimoto, N., Wehrli, C., Wiedensohler, A., and Zhang, X.-Y.: Recommendations for reporting "black carbon" measurements, Atmos. Chem. Phys., 13, 8365–8379, doi:10.5194/acp-13-8365-2013, 2013.

Pramanik, A., Kohler, J., Schuler, T.V., Van Pelt, W. and Cohen, L.: Comparison of snow accumulation events on two High-Arctic glaciers to model-derived and observed precipitation, Polar Res., 38, 3364, doi:10.33265/polar.v38.3364, 2019.

Proksch, M., Rutter, N., Fierz, C., and Schneebeli, M.: Intercomparison of snow density measurements: bias, precision, and vertical resolution, The Cryosphere, 10, 371–384, doi:10.5194/tc-10-371-2016, 2016.

Reistad, M., Breivik, Ø., Haakenstad, H., Aarnes, O. J. and Furevik, B. R.: *A high-resolution hindcast of wind and waves for the North Sea, the Norwegian Sea and the Barents Sea*, Tech. Rep. Met.No Rep. No. 2009/14, Norwegian Meteorological Institute, Oslo, 2009.

Rinke, A., Maturilli, M., Graham, R.M., Matthes, H., Handorf, D., Cohen, L. Hudson, S.R. and Moore, J.C.: Extreme cyclone events in the Arctic: Wintertime variability and trends, Environ. Res. Lett. 12, 094006, doi: 10.1088/1748-9326/aa7def, 2017.

Ruppel, M. M., Soares, J., Gallet, J.-C., Isaksson, E., Martma, T., Svensson, J., Kohler, J., Pedersen, C.A., Manninen, S., Korhola, A. and Ström, J.: Do contemporary (1980–2015) emissions determine the elemental carbon deposition trend at Holtedahlfonna glacier, Svalbard? Atmos. Chem. Phys., 17, 12,779–12,795, doi:10.5194/acp-17-12779-2017, 2017.

Ruppel, M. M., Isaksson, E., Ström, J., Beaudon, E., Svensson, J., Pedersen, C. A., and Korhola, A.: Increase in elemental carbon values between 1970 and 2004 observed in a 300-year ice core from Holtedahlfonna (Svalbard), Atmos. Chem. Phys., 14, 11447–11460, doi:10.5194/acp-14-11447-2014, 2014.

https://doi.org/10.5194/acp-2020-491
Preprint. Discussion started: 16 June 2020


Sinha, P. R., Kondo, Y., Goto-Azuma, K., Tsukagawa, Y., Fukuda, K., Koike, M., Oshima, N., Førland, E.J., Irwin, M., Gallet, J.-C., and Pedersen, C. A.: Seasonal progression of the deposition of black carbon by snowfall at Ny-Ålesund, Spitsbergen. J. Geophys. Res. Atmos., 123, 997–1016, doi: 10.1002/2017JD028027, 2018.

Sinha, P. R., Kondo, Y., Koike, M., Ogren, J. A., Jefferson, A., Barrett, T. E., Sheesley, R. J., Ohata, S., Moteki, N., Coe, H. Liu, D., Irwin, M., Tunved, P., Quinn, P. K. and Y. Zhao, Y.: Evaluation of ground-based black carbon measurements by filter-based photometers at two Arctic sites, J. Geophys. Res. Atmos., 122, 3544–3572, doi:10.1002/2016JD025843, 2017.

Spolaor, A., Barbaro, E., Mazzola, M., Viola, A.P., Lisok, J., Obleitner, F., Markowicz, K.M. and Cappelletti, D.: Determination of black carbon and nanoparticles along glaciers in the Spitsbergen (Svalbard) region exploiting a mobile platform, Atmos. Environ., 170: 184-196, doi: 10.1016/j.atmosenv.2017.09.042, 2017.

Stephens, M., Turner, N. and Sandberg, J.: Particle identification by laser-induced incandescence in a solid-state laser cavity. Appl. Opt., 42, 19, 3726–3736, doi: 10.1364/AO.42.003726, 2003.

Stohl, A., Aamaas, B., Amann, M., Baker, L. H., Bellouin, N., Berntsen, T. K., Boucher, O., Cherian, R., Collins, W., Daskalakis, N., Dusinska, M., Eckhardt, S., Fuglestvedt, J. S., Harju, M., Heyes, C., Hodnebrog, Ø., Hao, J., Im, U., Kanakidou, M., Klimont, Z., Kupiainen, K., Law, K. S., Lund, M. T., Maas, R., MacIntosh, C. R., Myhre, G., Myriokefalitakis, S., Olivié, D., Quaas, J., Quennehen, B., Raut, J.-C., Rumbold, S. T., Samset, B. H., Schulz, M., Seland, Ø., Shine, K. P., Skeie, R. B., Wang, S., Yttri, K. E., and Zhu, T.: Evaluating the climate and air quality impacts of short-lived pollutants, Atmos. Chem. Phys., 15, 10529–10566, doi:10.5194/acp-15-10529-2015, 2015.

Svensson, J., Ström, J., Kivekäs, N., Dkhar, N. B., Tayal, S., Sharma, V. P., Jutila, A., Backman, J., Virkkula, A., Ruppel, M., Hyvärinen, A., Kontu, A., Hannula, H.-R., Leppäranta, M., Hooda, R. K., Korhola, A., Asmi, E., and Lihavainen, H.: Light-absorption of dust and elemental carbon in snow in the Indian Himalayas and the Finnish Arctic, Atmos. Meas. Tech., 11, 1403–1416, doi:10.5194/amt-11-1403-2018, 2018.

Svensson, J. Ström, J., Hansson, M., Lihavainen, H., and Kerminen, V.-M.: Observed metre scale horizontal variability of elemental carbon in surface snow, Environ. Res. Lett., 8, 034012, doi:10.1088/1748-9326/8/3/034012, 2013.

Van Kampenhout, L., Lenaerts, J. T. M., Lipscomb, W. H., Sacks, W. J., Lawrence, D. M., Slater, A. G., and van den Broeke, M. R.: Improving the representation of polar snow and firn in the Community Earth System Model. J. Adv. Mod. Earth Sy., 9, 2583–2600, doi:10.1002/2017MS000988, 2017.

Van Pelt, W.J.J. and Kohler, J.: Modelling the long-term mass balance and firn evolution of glaciers around Kongsfjorden, Svalbard, J. Glaciol., 61, 228, doi:10.3189/2015JoG14J223, 2015.

Van Pelt, W., Pohjola, V., Pettersson, R., Marchenko, S., Kohler, J., Luks, B., Ove Hagen, J.O., Schuler, T.V., Dunse, T., Noël, B. and Reijmer. C.: A long-term dataset of climatic mass balance, snow conditions, and runoff in Svalbard (1957–2018), The Cryosphere, 13, 2259–2280, doi: 10.5194/tc-13-2259-2019, 2019.

https://doi.org/10.5194/acp-2020-491
Preprint. Discussion started: 16 June 2020


Atmospheric Chemistry and Physics
Discussions

Van Pelt, W.J.J., J. Oerlemans, C.H. Reijmer, V.A. Pohjola, R. Pettersson and J.H. van Angelen: Simulating melt, runoff and refreezing on Nordenskiöldbreen, Svalbard, using a coupled snow and energy balance model. The Cryosphere, 6, 641-659, doi:10.5194/tc-6-641-2012, 2012.

Vionnet, V., Brun, E., Morin, S., Boone, A., Faroux, S., Le Moigne, P., Martin, E., and Willemet, J.-M.: The detailed snowpack scheme Crocus and its implementation in SURFEX v7.2, Geosci. Model Dev., 5, 773–791, doi:10.5194/gmd-5-773-2012, 2012.

Wang , M., Xu, B., Zhao, H., Cao, J., Joswiak, D., Wu, G. and Lin, S.: The influence of dust on quantitative measurements of black carbon in ice and snow when using a thermal optical method, Aerosol Sci. Tech., 46, 1, 60-69, doi:10.1080/02786826.2011.605815, 2012.

Winiger, P., Barrett, T. E., Sheesley, R. J., Huang, L., Sharma, S., Barrie, L.A., Yttri, K. E., Evangeliou, N., Eckhardt, S., Stohl, A., Klimont, Z., Heyes, C., Semiletov, I.P., Dudarev, O. V., Charkin, A., Shakhova, N., Holmstrand, H., Andersson, A. and Gustafsson, Ö.: Source apportionment of circum-Arctic atmospheric black carbon from isotopes and modeling, Sci. Adv. 5, 2, eaau8052, doi:10.1126/sciadv.aau8052, 2019.

Winiger, P., Andersson, A., Yttri, K.E., Tunved, P. and Gutsfasson, Ö.: Isotope-based source apportionment of EC aerosol particles during winter high-pollution events at the Zeppelin Observatory, Svalbard, Environ. Sci. Technol., 49, 11959−11966, doi:10.1021/acs.est.5b02644, 2015.

Xu, B., Cao, J., Joswiak, D. R., Liu, X., Zhao, H., and He, J.: Postdepositional enrichment of black soot in snow-pack and accelerated melting of Tibetan glaciers, Environ. Res. Lett., 7, 014022, doi:10.1088/1748-9326/7/1/014022, 2012.

https://doi.org/10.5194/acp-2020-491
Preprint. Discussion started: 16 June 2020


Atmospheric Chemistry and Physics
Discussions

| Acronym or symbol | Units | Definition |
|---|---|---|
| BC | | Black carbon: Light-absorbing, refractory particulate carbon aerosols emitted by the incomplete combustion of organic fuels (biomass or fossil fuels). |
| TOT | | Thermo-optical transmittance method used to analyze particulate carbon in snow |
| EC | | Elemental carbon: Refractory fraction of particulate carbon in snow determined by TOT |
| OC | | Organic carbon: Volatile fraction of particulate carbon in snow determined by TOT |
| $C_{snow}^{EC}$ | ng g$^{-1}$ | Mass concentration of EC in snow determined by the TOT method |
| $C_{snow}^{OC}$ | ng g$^{-1}$ | Mass concentration of OC in snow determined by the TOT method |
| $\tilde{C}_{snow}^{EC}$ | ng g$^{-1}$ | Median value of $C_{snow}^{EC}$ |
| $\tilde{C}_{snow}^{OC}$ | ng g$^{-1}$ | Median value of $C_{snow}^{OC}$ |
| $L_{filt}^{EC}$ | µg cm$^{-2}$ | Mass loading of EC on filters determined by the TOT method |
| $L_{filt}^{OC}$ | µg cm$^{-2}$ | Mass loading of OC on filters determined by the TOT method |
| $h_{SWE}$ | cm | Snow depth expressed in water equivalent |
| $L_{snow}^{EC}$ | mg m$^{-2}$ | Mass loading of EC in the seasonal snowpack, based on measurements of $C_{snow}^{EC}$ |
| $L_{snow}^{OC}$ | mg m$^{-2}$ | Mass loading of OC in the seasonal snowpack, based on measurements of $C_{snow}^{OC}$ |
| eBC | | Equivalent black carbon: BC measured in air filters by light-absorption methods |
| PSAP | | Particle Soot Absorption Photometer used to measure eBC in air filters |
| $C_{air}^{eBC}$ | ng m$^{-3}$ | Mass mixing ratio of eBC in air, determined by light-absorption methods |
| $\tilde{C}_{air}^{eBC}$ | ng m$^{-3}$ | Median value of $C_{air}^{eBC}$ |
| $MAC_{\lambda}$ | m$^{2}$ g$^{-1}$ | Wavelength-dependent mass absorption coefficient of light by eBC |

**Table 1.** Main symbols and acronyms used in this paper. The various terms for black carbon (BC, EC, OC, eBC) are as defined in Petzold et al. (2013).

https://doi.org/10.5194/acp-2020-491
Preprint. Discussion started: 16 June 2020


Atmospheric Chemistry and Physics
Discussions

| | Spring 2016 glacier survey (22 sites) | | Austre Brøggerbreen 2007–18 (4 sites) | Other sites 2016–17 (21 sites) | Sverdrup & Gruvebadet 2010–18 (2 sites) |
|---|---|---|---|---|---|
| | All layers | Surface | Surface | Surface | Surface |
| **$C_{snow}^{EC}$ (ng g$^{-1}$)** | | | | | |
| *n* | 89 | 22 | 115 | 34 | 86 |
| *n** | 72 | 21 | 88 | 33 | 75 |
| Minimum | <1.0 | <1.0 | <1.0 | <1.0 | <1.0 |
| Maximum | 33.0 | 22.7 | 45.2 | 25.4 | 266.6 |
| Median | 2.0 | 2.4 | 3.3 | 6.2 | 9.7 |
| Mean | 3.0 | 4.5 | 5.5 | 7.2 | 25.8 |
| Geo. mean | 1.8 | 3.2 | 2.7 | 5.5 | 7.6 |
| **$C_{snow}^{OC}$ (ng g$^{-1}$)** | | | | | |
| *n* | 89 | 22 | 115 | 34 | 86 |
| *n** | 89 | 22 | 114 | 34 | 85 |
| Minimum | 11.9 | 21.2 | <1.0 | 18.0 | <1.0 |
| Maximum | 901.4 | 549.9 | 1076.2 | 3448.9 | 9449.1 |
| Median | 48.6 | 49.4 | 58.7 | 385.8 | 105.1 |
| Mean | 88.4 | 80.3 | 175.1 | 578.1 | 609.7 |
| Geo. mean | 60.5 | 56.9 | 53.3 | 288.3 | 91.3 |
| **EC/OC** | | | | | |
| Minimum | 0.01 | 0.02 | <0.01 | <0.01 | <0.01 |
| Maximum | 0.27 | 0.27 | 0.43 | 0.11 | 1.56 |
| Median | 0.04 | 0.04 | 0.04 | 0.02 | 0.13 |
| Mean | 0.06 | 0.08 | 0.08 | 0.03 | 0.21 |
| Geo. mean | 0.04 | 0.06 | 0.04 | 0.02 | 0.12 |

**Table 2.** Descriptive statistics for $C_{snow}^{EC}$, $C_{snow}^{OC}$ and EC/OC snow in samples analyzed in this study. $n^*$ is the number of values > 1 ng g$^{-1}$. Two outliers with $C_{snow}^{EC}$ >1700 ng g$^{-1}$ were excluded from calculations.

https://doi.org/10.5194/acp-2020-491
Preprint. Discussion started: 16 June 2020


Atmospheric Chemistry and Physics
Discussions

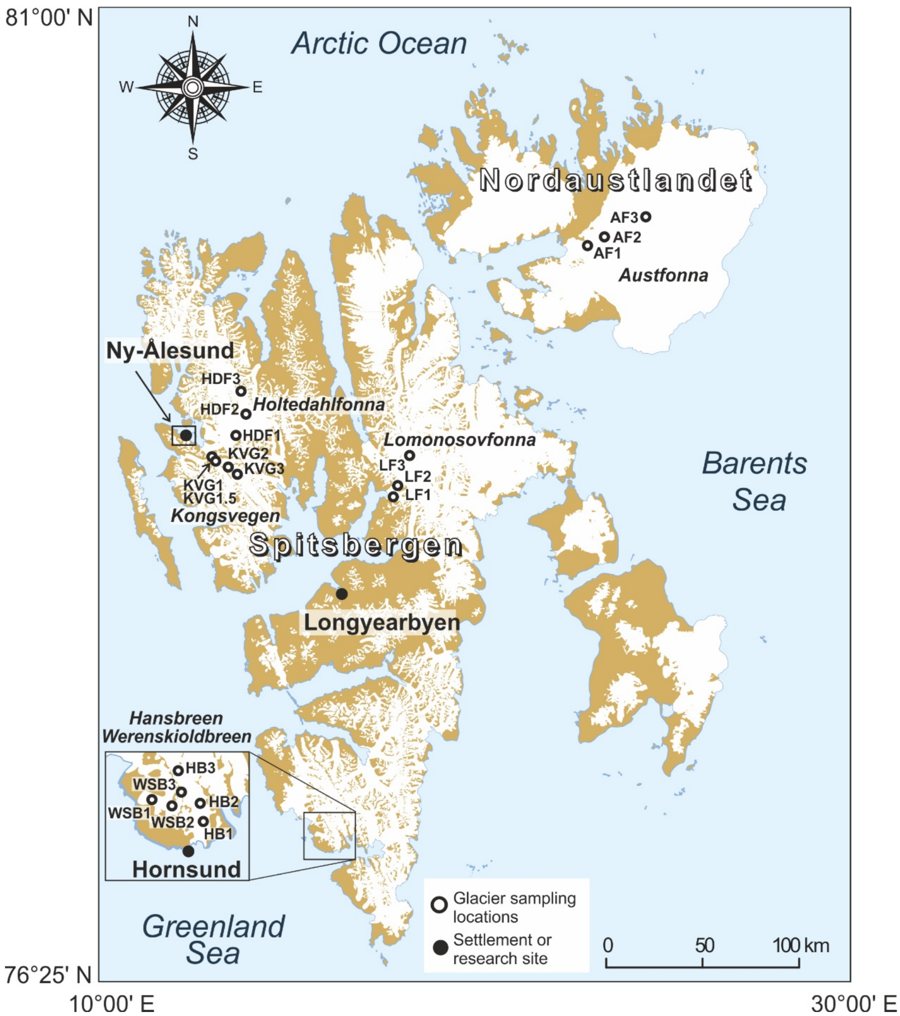


**Fig. 1.** Location map of the Svalbard archipelago, showing the glaciers where snow was sampled during the April 2016 survey. See **Fig. S2** for sampling sites near Ny-Ålesund on Brøgger Peninsula.

https://doi.org/10.5194/acp-2020-491
Preprint. Discussion started: 16 June 2020


Atmospheric Chemistry and Physics
Discussions

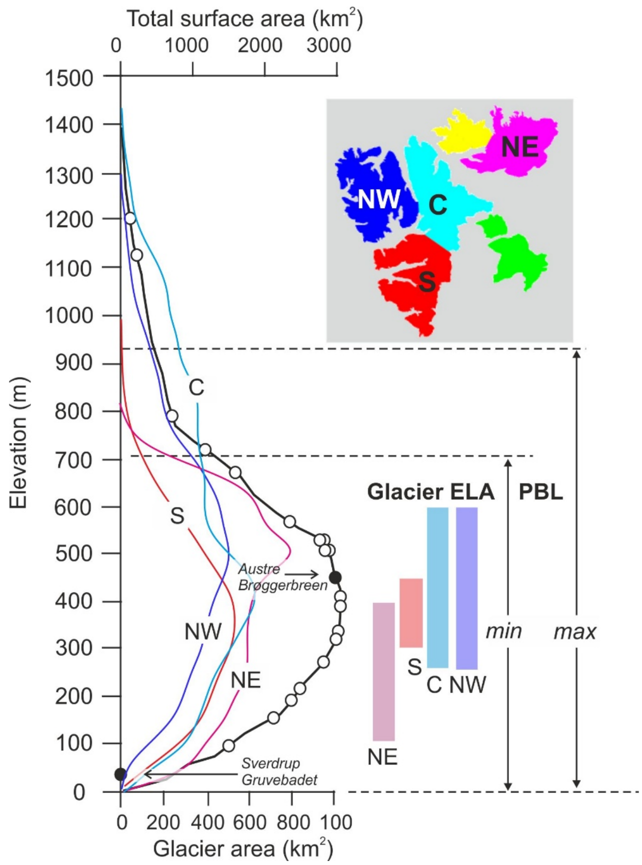


**Fig. 2.** Distribution of the Svalbard snow sampling sites with respect to elevation and surface hypsometry. Open circles are glacier sites sampled duringduring the April 2016 survey, while full circles are sites where surface snow was collected on the Brøgger Peninsula between 2007 and 2018. The thicker black line is the total area distribution over the archipelago (upper scale; from James et al., 2012), while the colored lines show the glacier hypsometry (lower scale) over southern (S), central (C), northeastern (NE) and northwestern (NW) Svalbard, as defined in König et al., 2014 (inset). Also shown are estimated ranges of the long-term mean Equilibrium Line Altitude (ELA; 1957–2018) for glaciers in each of the aforementioned sectors (van Pelt et al., 2019), and the minimum (winter) and maximum (summer) thickness of the Planetary Boundary Layer (PBL) in the maritime sector of the European Arctic, based on ERA-40 reanalysis over 1969–2001 (Esau and Sorokina, 2009).

https://doi.org/10.5194/acp-2020-491
Preprint. Discussion started: 16 June 2020


Atmospheric Chemistry and Physics
Discussions

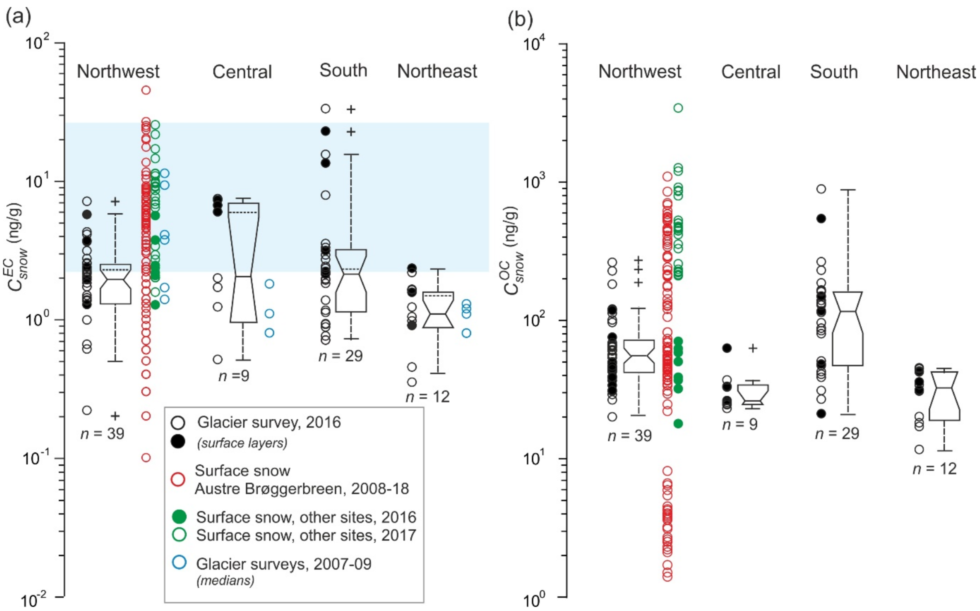


**Fig. 3.** Measurements of (a) $C_{snow}^{EC}$ and (b) $C_{snow}^{OC}$ on Svalbard glaciers, grouped by geographic sectors (defined on Fig. 2). The box-whisker plots only include snowpit measurements from glaciers surveyed in April 2016. Box heights give the interquartile range, and plus signs ("+") are outliers. Notches bracket the 95 % confidence limits on the median. The dotted horizontal traits on some box plots denote the medians when values <1 ng g$^{-1}$ are excluded. Values of $C_{snow}^{EC}$ and (b) $C_{snow}^{OC}$ measured in discrete snowpit layers are shown as black open circles, and filled circles correspond to surface layers. Also plotted for comparison are $C_{snow}^{EC}$ and $C_{snow}^{OC}$ in surface layers on Austre Brøggerbreen, 2007–18 (red circles) and at other sites, 2016–17 (green circles; **Table S2**). The median $C_{snow}^{EC}$ and $C_{snow}^{OC}$ measured on glaciers in 2007–09 (Forsström et al., 2013) are shown as blue circles. The blue shaded bar is the interquartile range of $C_{snow}^{EC}$ in surface layers of the tundra snowpack near Ny Ålesund, 2007–18 (this study).

https://doi.org/10.5194/acp-2020-491
Preprint. Discussion started: 16 June 2020


Atmospheric Chemistry and Physics
Discussions

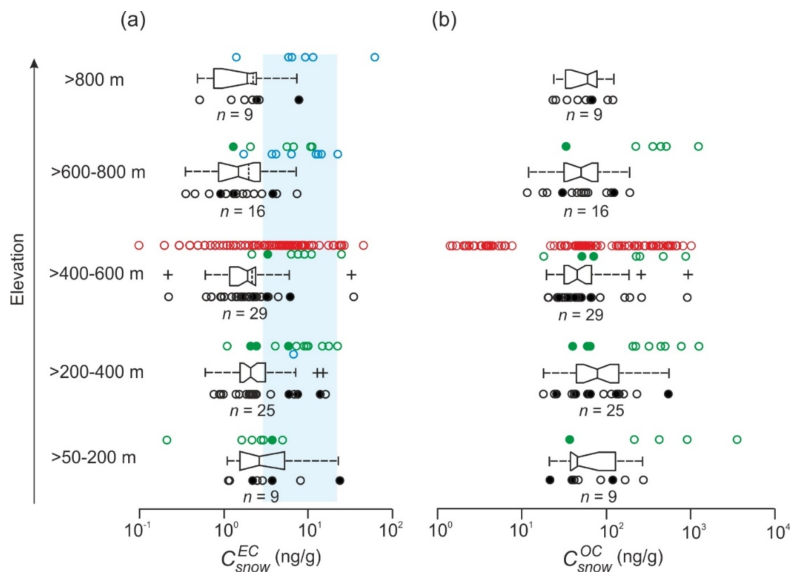


**Fig. 4.** Measurements of (a) $C_{snow}^{EC}$ and (b) $C_{snow}^{OC}$ on Svalbard glaciers, grouped into discrete elevation bins. Data symbols and box plots are defined as in **Fig. 3**.

https://doi.org/10.5194/acp-2020-491
Preprint. Discussion started: 16 June 2020


Atmospheric Chemistry and Physics
Discussions

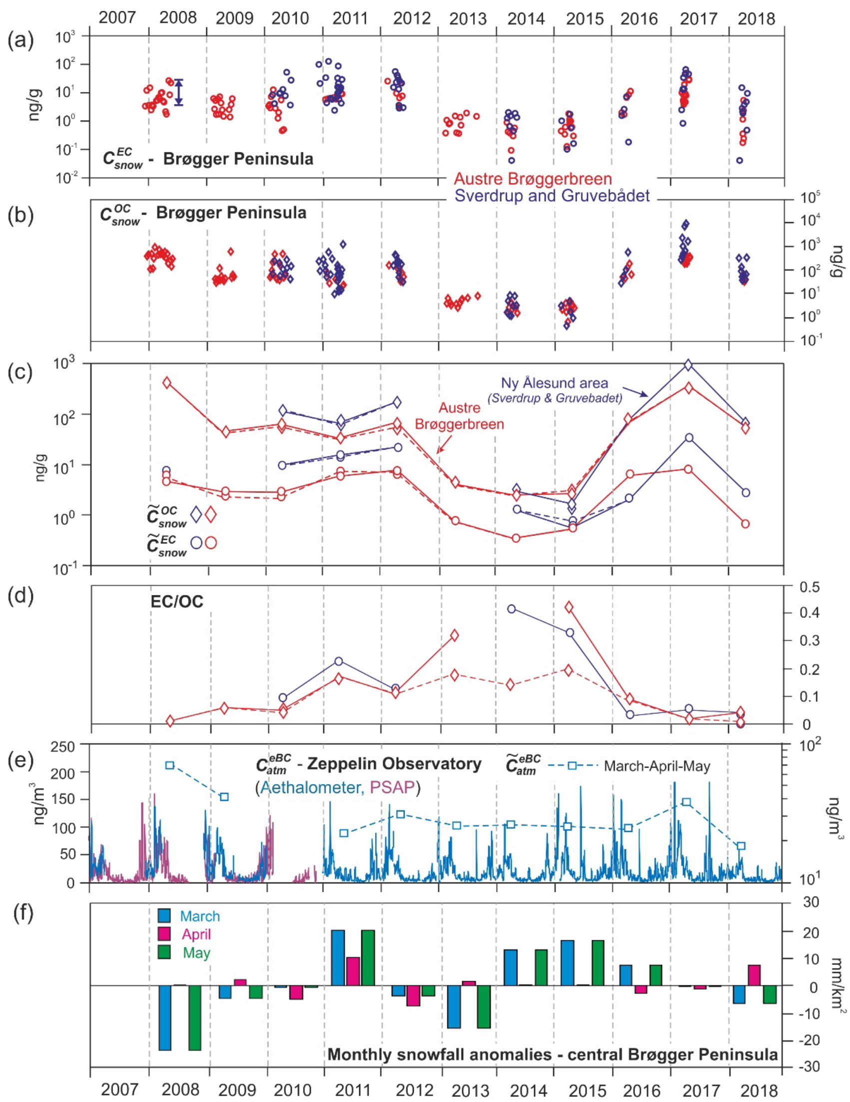


**Fig. 5.** (a) $C_{snow}^{EC}$ and (b) $C_{snow}^{OC}$ in surface layers on central Brøgger Peninsula, Svalbard, 2008–18. The double-headed arrow in (a) is the interquartile range of $C_{snow}^{EC}$ measured near Ny Ålesund in March 2008 by Aamaas et al. (2011). (c) and (d) Median values of $C_{snow}^{EC}$, $C_{snow}^{OC}$ and EC/OC including all data points (full lines), and for spring months only (MAM; stippled lines). (e) Weekly averages of $C_{atm}^{eBC}$ at Zeppelin Observatory, measured using two methods (Aethalometer, PSAP). The median for spring months ($\tilde{C}_{air}^{eBC}$) in each year is also displayed (stippled line; right-hand scale). (f) Area-averaged anomalies of total snowfall over central Brøgger Peninsula during spring months, simulated using the snowpack model (see **Fig. S3** for area boundaries).

https://doi.org/10.5194/acp-2020-491
Preprint. Discussion started: 16 June 2020




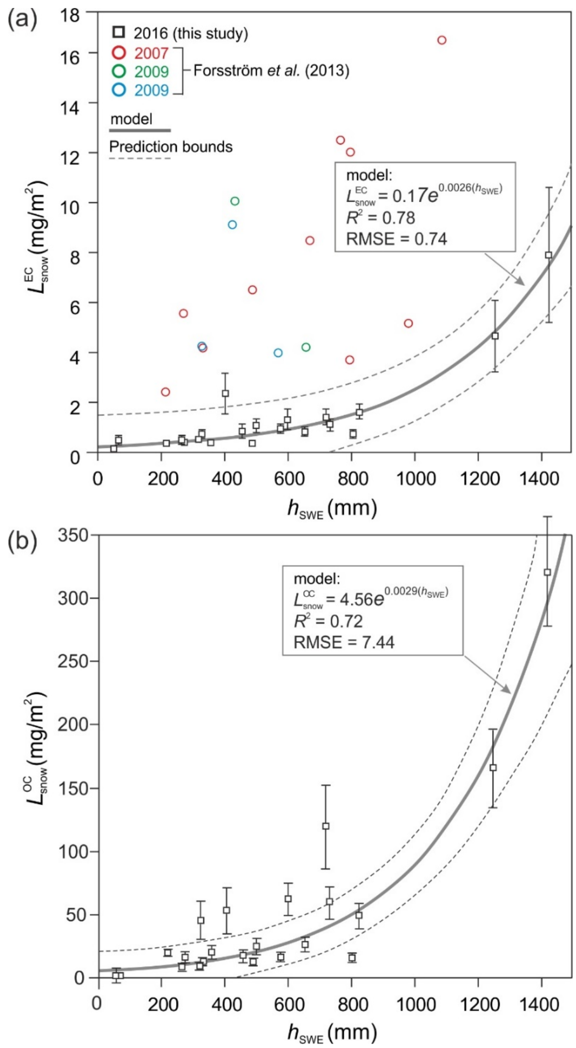


**Fig. 6.** Scatterplot of (a) $L_{snow}^{EC}$ and (b) $L_{snow}^{OC}$ against $h_{SWE}$ based on measurements from Svalbard glacier snowpits from the April 2016 survey. The error bars are ± 1σ, and take into account uncertainties in $h_{SWE}$, $C_{snow}^{EC}$, and $C_{snow}^{OC}$. An exponential model, shown with 95% confidence bounds on predictions, was fitted by nonlinear least-squares regression, inversely weighted against data errors. In panel (a), data from earlier surveys by Forsström et al. (2009, 2013) are displayed for comparison.

https://doi.org/10.5194/acp-2020-491
Preprint. Discussion started: 16 June 2020


Atmospheric Chemistry and Physics
Open Access
EGU
Discussions

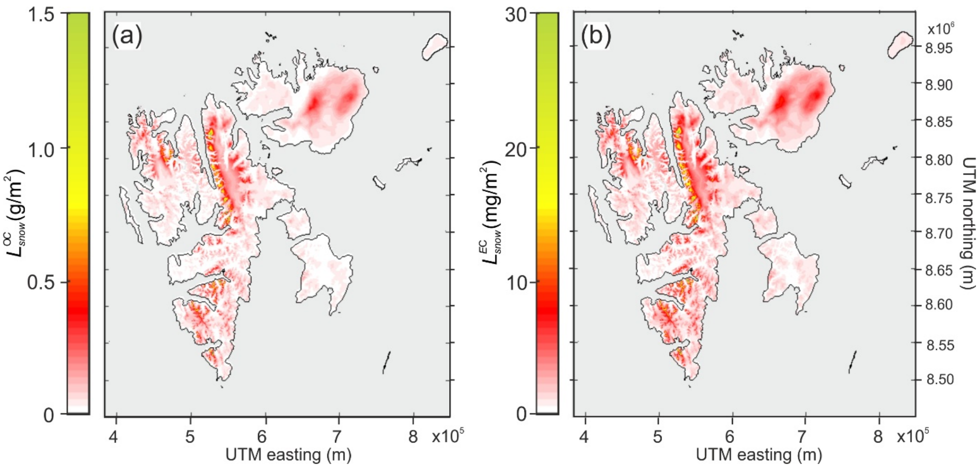


**Fig. 7.** Maps of (a) $L_{snow}^{OC}$ and (b) $L_{snow}^{EC}$ in the late winter 2015–16 snowpack over Svalbard, based on the empirical relationships shown in **Fig. 6**, applied to the map of $h_{\mathrm{SWE}}$ between 1 Sept. 2015 and 30 April 2016 generated using the snowpack model (Van Pelt et al. 2019). Note that these maps do not include EC and OC deposition in snow from local point sources of pollution around settlements such as Barentsburg, Longyearbyen or Ny-Ålesund.

https://doi.org/10.5194/acp-2020-491
Preprint. Discussion started: 16 June 2020


Atmospheric Chemistry and Physics
Discussions

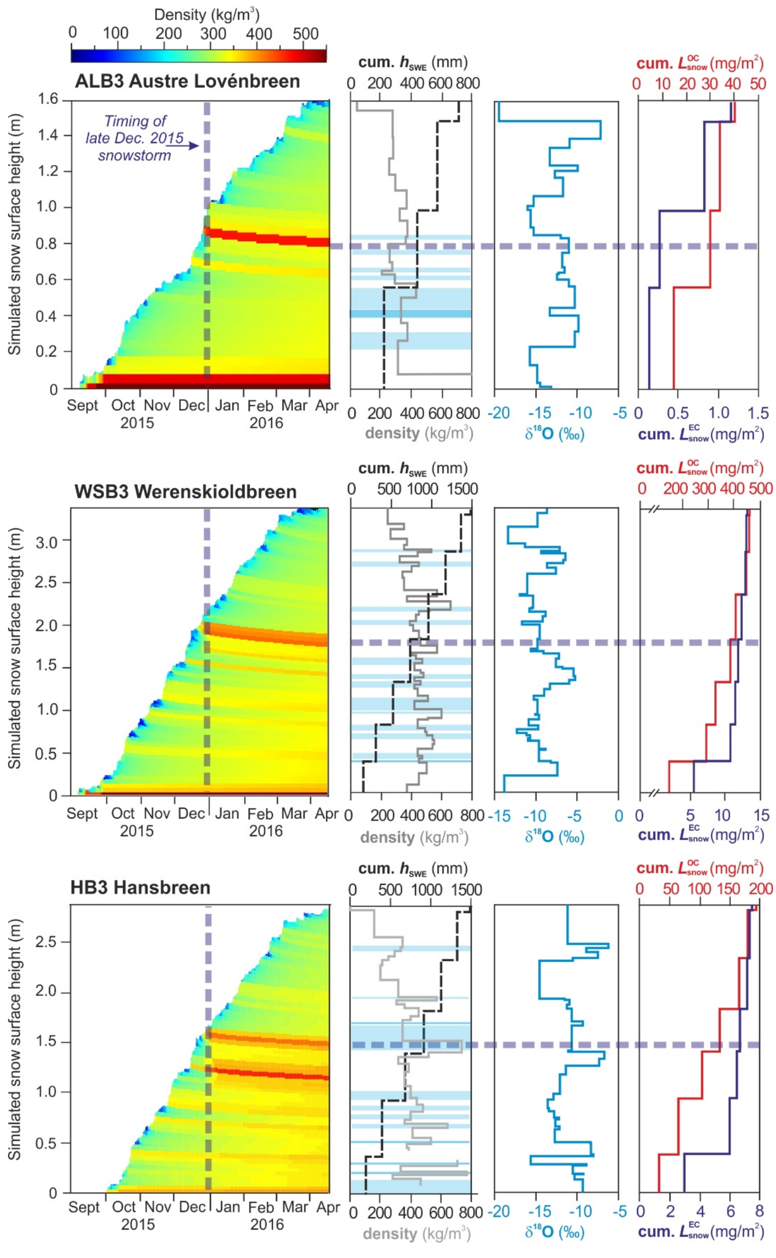


**Fig. 8.** Simulated evolution of the snowpack from Sept 2015 to April 2016 at three glacier sites on Spitsbergen, compared with measured profiles of density, cumulative $h_{\mathrm{SWE}}$, δ$^{18}$O, as well as cumulative $L^{EC}_{snow}$ and $L^{OC}_{snow}$ in the snowpack. The $h_{\mathrm{SWE}}$ over the EC and OC sampling intervals was computed using the discrete snow layer density data. Where density measurements were missing, values from comparable layers in other snowpits were used. Snow layers with $C^{EC}_{snow}$ <1 ng g$^{-1}$ were assigned a value of 0.5 ng g$^{-1}$ for $L^{EC}_{snow}$ calculations. Icy snow and discrete ice layers are shown as pale and darker blue lines, respectively.

https://doi.org/10.5194/acp-2020-491
Preprint. Discussion started: 16 June 2020


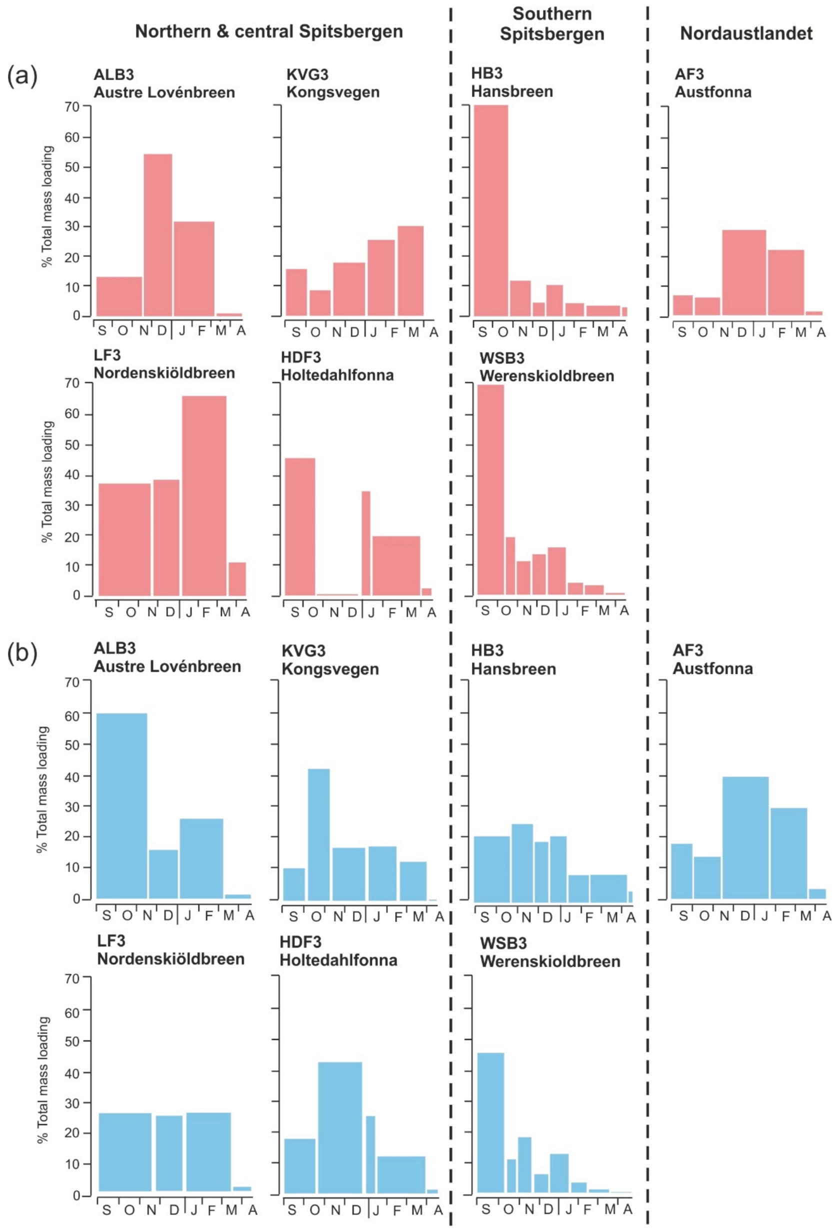


**Fig. 9.** Sub-seasonal increments of (a) $L_{snow}^{EC}$ and (b) $L_{snow}^{OC}$ on Svalbard glaciers during the 2015–16 winter, as estimated using the snowpack model (e.g., **Fig. 8**).

https://doi.org/10.5194/acp-2020-491
Preprint. Discussion started: 16 June 2020



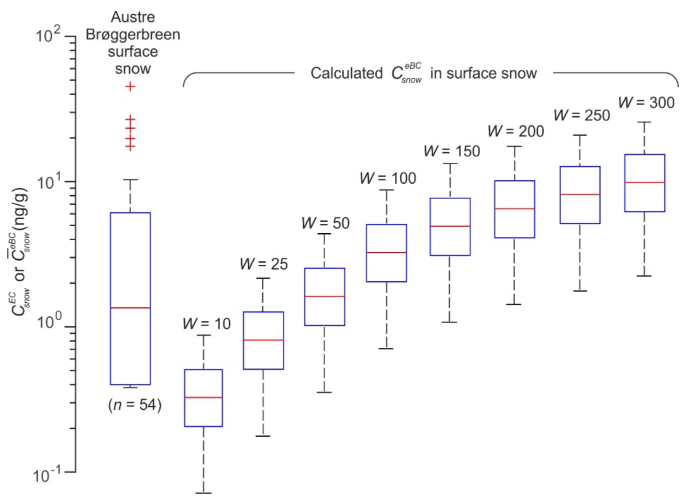


**Fig. 10.** Box-whisker plot of $C_{snow}^{EC}$ measured in surface layers on Austre Brøggerbreen in the spring months of 2011–18 (far left), compared with box-whisker plots of mean $C_{snow}^{EC}$ calculated from $C_{air}^{eBC}$ at Zeppelin Observatory, and using different values of the snow washout ratio $W$. Red plus signs (+) are outliers.

https://doi.org/10.5194/acp-2020-491
Preprint. Discussion started: 16 June 2020


Atmospheric Chemistry and Physics Discussions

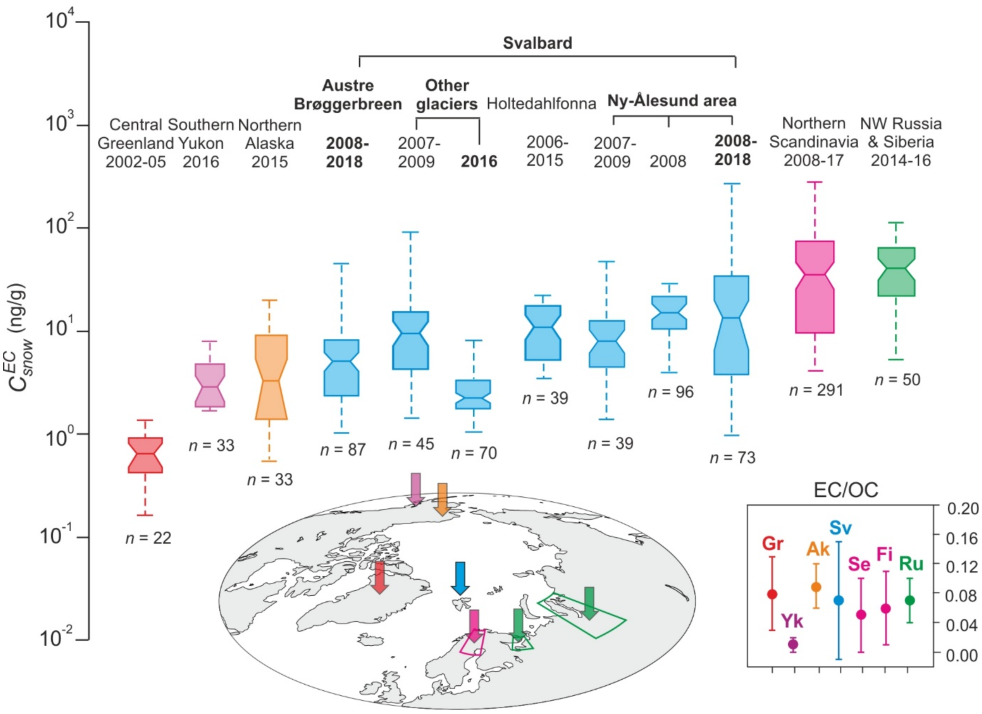


**Fig. 11.** Measurements of $C_{snow}^{EC}$ on Svalbard reported in this study (bold headers; values >1 ng g$^{-1}$), compared with winter/spring snowpack data from other circum-Arctic sites, color-coded by region. Inset at far right: mean EC/OC (± s.d.) in snow from regions identified in the plot: Greenland (Gr), Yukon (Yk), Svalbard (Sv), Sweden (Se), Finland (Fi) and Russia (Ru). Only data obtained by thermo-optical analysis are included, although protocols differ between studies (see **Table S4**). The box-whisker plots are as defined in **Fig. 3**, but outliers were removed for clarity. Published data sources for Svalbard glaciers: Forsström et al. (2009, 2013) and Ruppel et al. (2017); Ny-Ålesund and Longyearbyen: Aamaas et al. (2011); Greenland: Hagler et al. (2007); Alaska: Dou et al. (2007); northern Scandinavia: Forsström et al. (2013), Meinander et al. (2013), Svensson et al. (2013, 2018), and unpublished data (**Table S5**); Russia and Siberia: Evangeliou et al. (2018); Yukon and Sweden: unpublished data (**Table S5**). Data from Greenland and the Yukon span 3–6 years of accumulation in snow, while data from Holtedahlfonna span an estimated ~8 years (2006–14). Five samples with $C_{snow}^{EC}$ > 140 ng g$^{-1}$ taken in Russian towns (Tomsk, Archangelsk) were excluded from the dataset by Evangeliou et al. (2018).